Schweizerische Eidgenossenschaft
Confédération suisse
Confederazione Svizzera
Confederaziun svizra

Federal Department of the Environment, Transport, Energy and Communications DETEC

Swiss Federal Office of Energy SFOE
Energy Research and Cleantech Division

Final report dated 31. March 2021

SiCUm: Fundamentals of an Efficient Low Voltage SiC Converter

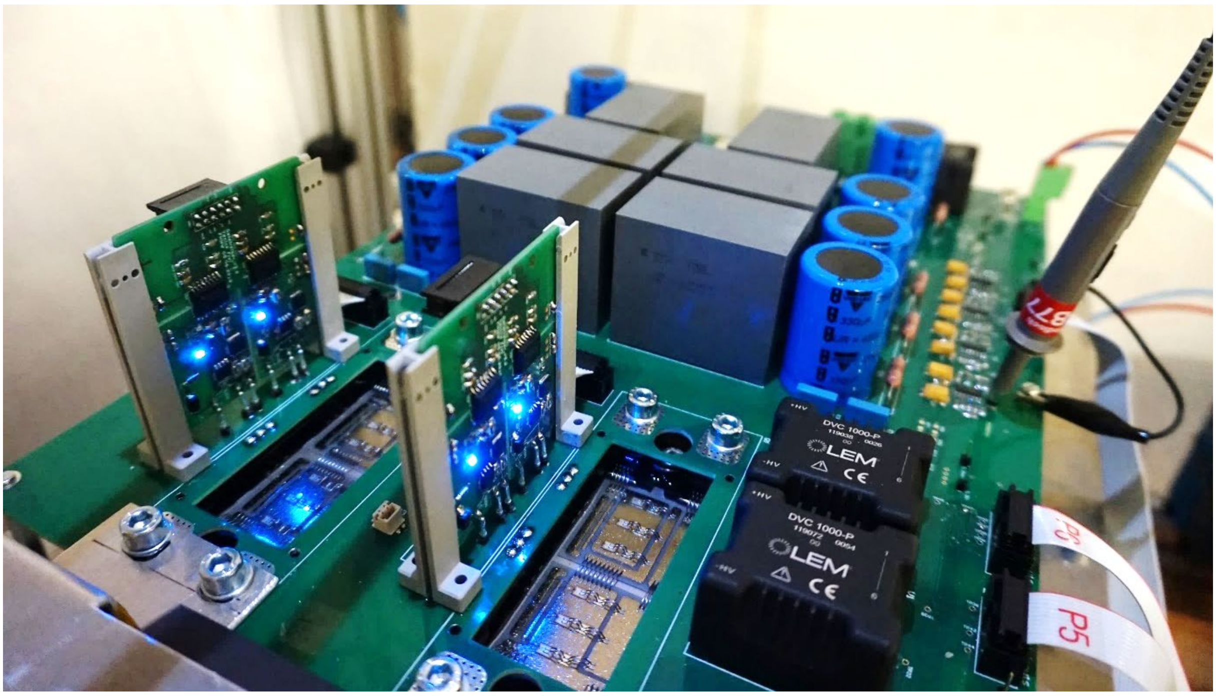

Source: ©FHNW Institute of Electric Power Systems 2021

Fachhochschule Nordwestschweiz
Hochschule für Technik

Date: 31. March 2021

Location: Bern

Publisher:
Swiss Federal Office of Energy SFOE
Energy Research and Cleantech
CH-3003 Bern
www.bfe.admin.ch

Subsidy recipients:
FHNW, Hochschule für Technik
Klosterzelgstrasse 2
CH-5210 Windisch
www.fhnw.ch

OST Ostschweizer Fachhochschule
Oberseestrasse 10
CH-8640 Rapperswil
www.ost.ch

Authors:
Tobias Strittmatter, FHNW, tobias.strittmatter@fhnw.ch
Dr. Paula Diaz Reigosa, FHNW, paula.diazreigosa@fhnw.ch
Prof. Dr. Nicola Schulz, FHNW, nicola.schulz@fhnw.ch

SFOE project coordinators:
SFOE head of domain: Dr. Michael Moser, michael.moser@bfe.admin.ch
SFOE programme manager: Roland Brüniger, roland.brueniger@brueniger.swiss

SFOE contract number: SI/501732-01

Zusammenfassung

Ein Dual Active Bridge (DAB) DC/DC-Wandler, basierend auf SiC MOSFETs als aktive Halbleiterschalter, wurde entwickelt, aufgebaut und vollständig charakterisiert. Der DAB-Konverter ist kompatibel zu einem aktiven Gleichrichter, der von der Ostschweizer Fachhochschule OST in einem Parallelprojekt entwickelt wurde.

Die gesamte Topologie besteht aus einem Eingangs-EMV-Netzfilter, einem dreiphasigen aktiven Gleichrichter, dem Zwischenkreis und dem DAB-Konverter, der für eine galvanische Trennung sorgt. Der Aufbau bietet die Möglichkeit eines bidirektionalen Leistungsflusses. Daher ermöglicht die Flexibilität dieser Topologie nicht nur einen geeigneten Anschluss mit galvanischer Isolation und bidirektionalem Leistungsfluss der Batterien von Elektrofahrzeugen ans Netz, sondern auch den Anschluss eines beliebigen DC-Busses an das Netz.

Die Spezifikationen des DAB-Konverters sind: Ausgangsleistung 22 kW; Zwischenkreisspannung (= Primärseite): 750 V; Ausgangsgleichspannung (= Sekundärseite): 320...450 V; MOSFET-Schaltfrequenz: 70 kHz.

Der Umrichter besteht aus zwei Hauptplatinen (PCB): Die erste Platine enthält den AC-Eingang und den 3-Phasen-Stromrichter (Teile der OST), die Zwischenkreiskondensatoren, die primärseitige H-Brücke des DAB-Konverters und die für die Regelung notwendigen Spannungs-/Strommessungen. Die zweite Platine beinhaltet die Sekundärseite des DAB-Konverters, Ausgangskondensatoren, den DC-Ausgang zur Last und weitere Spannungs-/Strommessungen. Beide Platinen sind für einen modularen Konverteraufbau identisch aufgebaut und werden über eine Serieninduktivität und einen Transformator verbunden, die beide von einem externen Lieferanten bezogen wurden. Die Ansteuerung der MOSFETs wurde mit bewährten Regelverfahren realisiert.

Der DAB-Konverter wurde hinsichtlich seines Wirkungsgrades in verschiedenen Betriebspunkten umfassend charakterisiert. Der höchste gemessene Gesamtwirkungsgrad liegt bei 95,58 %. Es hat sich herausgestellt, dass der grösste Teil der Konverterverluste durch die magnetischen Komponenten (d.h. die Drossel und den Transformator) entsteht. Die Halbleiterverluste des DAB-Konverters machen lediglich 1 % der übertragenen Leistung aus. Da die magnetischen Komponenten einen erheblichen Einfluss auf die Gesamtverluste des Konverters haben, wird empfohlen, die Optimierung der magnetischen Komponenten für den Betrieb über 50 kHz weiter zu untersuchen.

Der SiC-DAB-Konverter kann nicht direkt mit einem siliziumbasierten System verglichen werden, da die Schaltfrequenz von 70 kHz von vergleichbaren Si IGBTs nicht erreicht würde. Bei einem Betrieb mit 10 kHz Schaltfrequenz, was für SiC-MOSFETs eher niedrig, für Si-IGBTs aber besser geeignet ist, wären die Halbleiterverluste nochmals niedriger. Dagegen wären die Halbleiterverluste in einem Si-DAB-Konverter bei 10 kHz Schaltfrequenz um den Faktor Drei höher als bei SiC. Insbesondere im Teillastbereich wird der Wirkungsgradvorteil von SiC noch deutlicher.

Weiterhin wurde ein Zuverlässigkeitsmodell für DAB-Konverter erstellt und für den entwickelten Konverter angewendet. Aus einem Lastprofil für den Einsatz des Konverters berechnet das Modell die Temperaturprofile aller Halbleiterchips, welche dann zur Abschätzung der Halbleiter-Lebensdauern verwendet werden. Für den vorliegenden DAB-Konverter hat das Modell ergeben, dass die MOSFETs auf der Sekundärseite aufgrund einer höheren Strombelastung stärker beansprucht werden was eine reduziertere Lebensdauer prognostiziert. Im konkreten Anwendungsbeispiel des Konverters als bidirektionales Ladegerät wird aufgezeigt, dass auch die MOSFETs auf der Sekundärseite ausreichend dimensioniert sind, um einen zuverlässigen Langzeitbetrieb zu gewährleisten. Das Zuverlässigkeitsmodell kann zur Optimierung des Umrichterdesigns im Hinblick auf dessen Zuverlässigkeit und Auslegung genutzt werden, bevor der Umrichter gebaut wird. Ausserdem kann es auch für andere Topologien angepasst werden.

Mit den gewonnenen Erkenntnissen konnten bereits Folgeprojekte im Bereich der SiC-Umrichterentwicklung und SiC-Zuverlässigkeit in Zusammenarbeit mit der Industrie gestartet werden.

Résumé

Un convertisseur DC/DC double pont (DAB), basé sur des MOSFETs SiC, a été développé, construit et entièrement caractérisé. Le convertisseur DAB est compatible avec un redresseur, qui a été développé par l'Ostschweizer Fachhochschule OST dans un projet parallèle.

La topologie se compose d'un filtre d'entrée, d'un redresseur actif triphasé, d'un circuit intermédiaire de tension et du convertisseur DAB qui assure une isolation galvanique. La configuration offre la possibilité d'un flux de puissance bidirectionnel. Par conséquent, la flexibilité de cette topologie permet non seulement une connexion des batteries des véhicules électriques au réseau, mais aussi la connexion de n'importe quel bus DC au réseau avec une isolation galvanique et un flux d'énergie bidirectionnel.

Les spécifications du convertisseur DAB sont les suivantes : puissance de sortie de 22 kW ; tension du circuit intermédiaire de tension (= côté primaire) : 750 V ; tension de sortie DC (= côté secondaire) : 320…450 V ; fréquence de commutation MOSFET : 70 kHz.

Le convertisseur se compose de deux cartes de circuits imprimés (PCB) principales : La première carte comprend l'entrée AC et le redresseur actif triphasé à deux niveaux (partie OST), les condensateurs du circuit intermédiaire de tension, le pont en H côté primaire du convertisseur DAB et les mesures de tension/courant nécessaires au contrôle. La deuxième carte comprend le côté secondaire du convertisseur DAB, les condensateurs de sortie, la sortie DC vers la charge et d'autres mesures de tension/courant. Les deux circuits imprimés sont identiques pour une conception modulaire du convertisseur et sont connectés via une inductance en série et un transformateur. La commande des MOSFETs a été réalisée au moyen de topologies de commande éprouvées.

Le convertisseur DAB a été entièrement caractérisé en ce qui concerne son efficacité à différents points de fonctionnement. Le rendement total mesuré le plus élevé est de 95,58 %. Mais la plus grande partie des pertes du convertisseur vient des composants magnétiques (c'est-à-dire l'inductance et le transformateur). Les pertes de semi-conducteurs du convertisseur DAB ne représentent que 1%. Si l'on ne tient compte que des pertes dans les semi-conducteurs, le rendement de la DAB atteindrait 99 %. Comme les composants magnétiques ont un impact important sur les pertes totales du convertisseur, il est recommandé d'étudier en plus l'optimisation des composants magnétiques.

Le convertisseur DAB au SiC ne peut pas être comparé directement à un système au silicium, car la fréquence de commutation de 70 kHz n'est pas atteinte par des IGBT au Si comparables. Dans une fréquence de 10 kHz, un convertisseur DAB SiC atteindrait un rendement maximal supérieur à 99 %, alors qu'un convertisseur DAB Si n'atteindrait que 97 % (dans les deux cas seulement les pertes de semi-conducteurs sont prises en compte). En particulier, en régime de charge partielle, l'avantage du SiC en termes de rendement est encore plus marqué.

En plus, un modèle de fiabilité pour les convertisseurs DAB a été établi et appliqué au convertisseur développé. À partir d'un profil de charge dans l'entrée du convertisseur, le modèle calcule la température de jonction de tous les semi-conducteurs. Les températures sont ensuite utilisées pour estimer la durée de vie des semi-conducteurs. Pour le convertisseur DAB présenté, le modèle a révélé que les MOSFET du côté secondaire sont plus chargés, ce qui laisse prédire une durée de vie réduite. Dans l'exemple concret d'application du convertisseur comme chargeur bidirectionnel, il est démontré que les MOSFET du côté secondaire sont également suffisamment dimensionnés pour assurer un fonctionnement fiable à long terme. Le modèle de fiabilité peut être utilisé pour optimiser le convertisseur en termes de fiabilité dans la phase de conception, et il peut être adapté à d'autres types de convertisseurs.

Sur la base des résultats de ce projet, plusieurs projets de R&D dans le domaine du développement des convertisseurs SiC et de la fiabilité du SiC ont été lancés en coopération avec l'industrie.

Summary

A Dual Active Bridge (DAB) DC/DC converter, based on SiC MOSFETs as active semiconductor switches has been developed, built and fully characterized. The DAB converter is compatible to an active rectifier, which was developed by the Ostschweizer Fachhochschule OST in a parallel project.

The entire topology consists of an input EMC mains filter, a three-phase active rectifier, a DC link and the DAB converter which provides galvanic isolation. The setup features the possibility of bidirectional power flow. Hence, the flexibility of this topology enables not only a grid connection suitable for EV batteries, but for any DC bus to be connected to the mains with galvanic isolation and bidirectional power flow.

The DAB converter specifications are: output power 22 kW; DC link (= primary side) voltage: 750 V; DC output (= secondary side) voltage: 320…450 V; MOSFET switching frequency: 70 kHz.

The converter consists of two main printed circuit boards (PCB): The first board includes the AC input and the 3-phase two-level active rectifier (OST part), DC-link capacitors, the primary side H-bridge of the DAB converter and voltage/current measurements needed for control. The second board includes the secondary side of the DAB converter, output capacitors, the DC output to the load and further voltage/current measurements. Both PCBs are identical for a modular converter design and are connected via a series inductance and a transformer, which both had been purchased from an external supplier. The control of the MOSFETs has been realized by means of proven control topologies.

The DAB converter has been comprehensively characterized with respect to its efficiency at different operating points. The highest measured total efficiency is 95.58 %. It has turned out that the biggest part of the converter losses arises from the magnetic components (i.e., the choke and the transformer). The semiconductor losses of the DAB converter make up only 1 % of the transferred power. Since the magnetic components have a significant impact on the total converter losses, it is recommended to further investigate the optimization of magnetic components to be operated above 50 kHz.

The SiC DAB converter cannot directly be compared to a silicon-based system, since the switching frequency of 70 kHz is not reached by comparable Si IGBTs. When operated at 10 kHz - which is rather low for SiC MOSFETs but more suitable for Si IGBTs, a SiC DAB converter would reach a maximum efficiency above 99%; whereas a Si DAB converter would reach only 97 % (in both cases: only semiconductor losses considered). In particular in partial load regime, the efficiency benefit of SiC becomes even more pronounced.

Furthermore, a reliability model for DAB converters has been established and applied to the developed converter. From an input mission profile of the converter, the model calculates the junction temperature profiles of all semiconductors, which are then used to estimate the semiconductor lifetimes. For the present DAB converter, the model showed that the MOSFETs on the secondary side are more stressed due to a higher current load, which predicts a reduced lifetime. In the specific application example of the converter as a bidirectional charger, it is shown that the MOSFETs on the secondary side are also sufficiently dimensioned to ensure reliable long-term operation. The reliability model can be used to optimize converter design with respect to reliability and designing before the converter is physically built, and it can be adapted to other converter types.

With the knowledge gained, follow-up projects in the field of SiC converter development and SiC reliability could already be started in cooperation with industry.

Contents

Abbreviations

AC	Alternating Current
DAB	Dual Active Bridge
DC	Direct Current
EV	Electric Vehicle
EMC	Electro Magnetic Compatibility
FHNW	Fachhochschule Nordwestschweiz
IGBT	Insulated Gate Bipolar Transistor
IEE	Institut für Elektrische Energietechnik, Institute of Electric Power Systems
MOSFET	Metal-Oxide Semiconductor Field Effect Transistor
OST	Ostschweizer Fachhochschule
PCB	Printed Circuit Board
PFC	Power Factor Correction
SFOE	Swiss Federal Office of Energy
Si	Silicon
SiC	Silicon Carbide
SoC	State of Charge
THD	Total Harmonic Distortion
V2G	Vehicle-to-Grid

1 Introduction

1.1 Background information and current situation

An efficient and reliable converter, based on silicon carbide (SiC) technology, has been developed in a joint project between the University of Applied Sciences Northwestern Switzerland (FHNW) and the Eastern Switzerland University of Applied Sciences (OST). The AC/DC converter can be applied e.g. as a 22 kW bidirectional battery charger for electric vehicles. The purpose of the bi-directionality is to use the Electric Vehicle (EV) in a vehicle-to-grid (V2G) system designed for residential applications, where the EV can serve as storage unit. Especially for on-board chargers, where size and weight play an important role, the development effort is typically aimed at increasing the power-handling capability, efficiency increase and compactness. In the frame of this project, the main focus is to quantify the efficiency increase in respect to silicon-based chargers, however, the compactness has been also taken into consideration by selecting SiC devices that can switch at high frequencies and allowing smaller magnetic components. Nevertheless, the prototype designed in this project is not size and weight-optimized, since this was not the main goal of the project.

The proposed converter topology is presented in Figure 1. It consists of an AC/DC stage with an EMC mains filter and a DC/DC stage. At the OST, the AC/DC part is developed, being a three-phase two-level active rectifier topology. At the FHNW, the DC/DC part is designed and implemented, whose topology is a galvanic isolated Dual Active Bridge (DAB) converter [1]. This topology consists of a full bridge converter a series inductance, a transformer and again a full bridge converter on the secondary side of the transformer. Both high reliability and high efficiency are important for the converter, for which reason the goal was to use commercial components only. The design of the converter has been simulated with a model in the software PLECS. There, the power losses of the power semiconductor modules are calculated and can be compared for any of the operation points. Additionally, the model has been extended and coupled with a Python script, which calculates the efficiency and expected lifetime of the SiC power modules for a given application and load profiles.

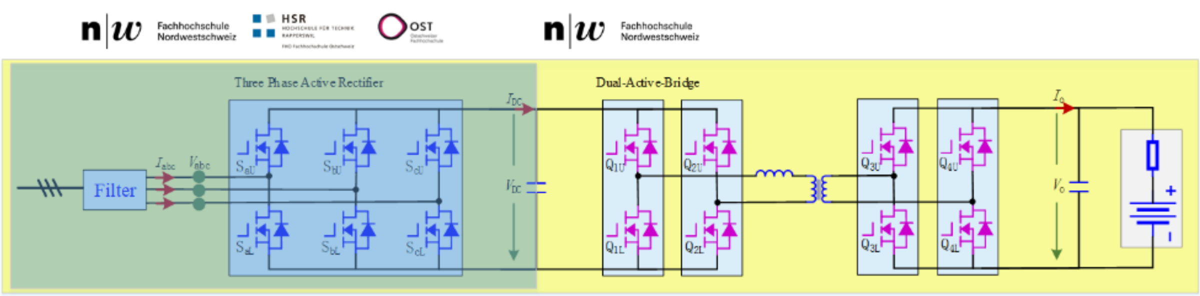

Figure 1: Schematic of the 22 kW three-phase bidirectional AC/DC SiC-based power converter. Green part: active rectifier developed by OST; yellow part: DAB converter developed by FHNW.

1.2 Purpose of the project

The aim of the project was to design, build and test an AC/DC power conversion system with a power rating of 20-30 kW at approx. 400-500 V output voltage. The inverter specifications should be comparable to existing converters using Si semiconductors, such that its efficiency can be compared to that of Si-based systems. Besides a high efficiency, the converter should also have a high reliability. For this purpose, the power converter has been built with off-the-shelf components (magnetic components, SiC semiconductor modules etc.) only, except the gate drivers which have been developed in-house at the IEE. A significant innovation of this AC/DC converter is the fact that only SiC semiconductor devices are used, with the aim of achieving high efficiency.

The power converter consists of the following stages: an active rectifier, a DC link and a DC/DC converter. The control strategy of the switches is realized by means of well-known control techniques [1,2]. The converter efficiency has been measured and calculated at different operating points. A comparison to Silicon-based systems is given. The reliability of the converter has been investigated by applying a given mission profile, which results in a specific semiconductor junction temperature profile and thus lifetime.

1.3 Objectives

This project has the following objectives:

- Assessment and selection of SiC semiconductor devices available on the market in terms of price, electrical properties and reliability data and selection of other power electronic components.
- Design and layout of the power electronic circuits with regard to high efficiency and operation at high switching frequency of the SiC MOSFETs (50 - 70 kHz).
- Set-up, commissioning and characterization of the SiC converter function pattern with regard to efficiency, thermal behaviour and reliability.
- Efficiency comparison (similar to the round robin test method for converter losses in drive systems) between a conventional Si converter and the SiC-based converter developed in this project. Literature data from the Si-based converter or simulations can also be used for such a comparison.
- Contacting and integration of possible project partners from the power electronics or drive sector.

2 Description of facility, procedures and methodology

A bidirectional battery charger for electrical vehicles is considered as target application. The decision has been made based on the promising trends in the automotive industry [3], where the charger plays a critical role in the deployment of battery-powered vehicles [4]. It is interesting to use SiC technology with the aim of increasing converter efficiency and lower battery charging times, while at the same time reducing overall size and weight.

For the AC/DC bi-directional stage, a three-phase two-level topology based on SiC power MOSFETs has been selected by OST. Details will be given in a separate report of the co-project SiCAa and therefore no further details are given in this report.

For the DC/DC stage, the Dual Active Bridge (DAB) topology is selected, since it is a common topology for EV chargers and its comparison with DABs using Si-semiconductors is possible [5-8]. The characteristics of the DAB, developed in this project are summarized in Table 1.

Table 1: Main characteristics of the Dual Active Bridge (DAB) converter developed in this project.

V_{in}	DC link voltage input (primary side)	750 V
V_{Out}	DC link voltage output (secondary side)	320 V – 450 V (typical EV battery voltage)
P_{Out}	Average power	22 kW
f_{sw}	Switching frequency range	50 -70 kHz
n_T	Transformer turns ratio In / Out	0.6
L_s	Total series / leakage inductance	21 µH
I_{in}	DC link current input (primary side)	45 Arms; 70 A peak
I_{Out}	DC link current output (secondary side)	75 Arms; 116 A peak

2.1 Selection of the magnetic components

The power that is being transferred between the primary and secondary H-bridges in the DAB converter topology depends on the value of the total series inductance between the bridges. Therefore, the phase shift angle between the generated rectangular voltages of the primary and secondary H-bridge, their amplitude and the transferred power of the converter is varied to define which is the maximum allowed total series inductance. For the calculation, the output voltage and the transformer ratio have been defined in Table 1. A surface plot is shown below for different power ratings and phase shift angles between the two rectangular voltages, resulting when the two H-bridges are switched at 70 kHz.

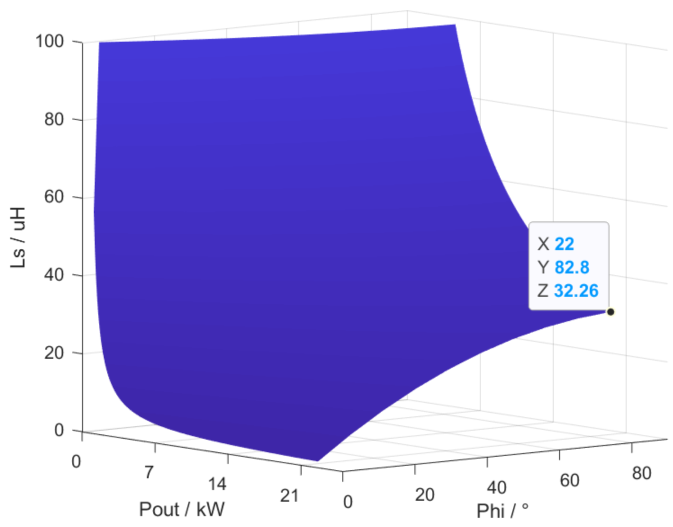

Figure 2: Maximum allowed series inductance (z-axis) as a function of the transferred power (x-axis) and phase angle (y-axis). The marked data point shows the maximum transferable power of 22 kW with a 32 µH total series inductance and a phase shift of 82.8°.

The data in Figure 2 shows the transferable power in function of the phase shift and the total series inductance of a DAB converter topology. For the developed converter an inductance of 21 µH has been specified. For all expected battery voltages the nominal power shall be transferable including margin. The power transfer curves for the 21 µH inductance and different battery voltages are calculated and shown in Figure 3. Even with 320 V battery voltage there is enough margin in the phase shift to be able to transfer more than the nominal power.

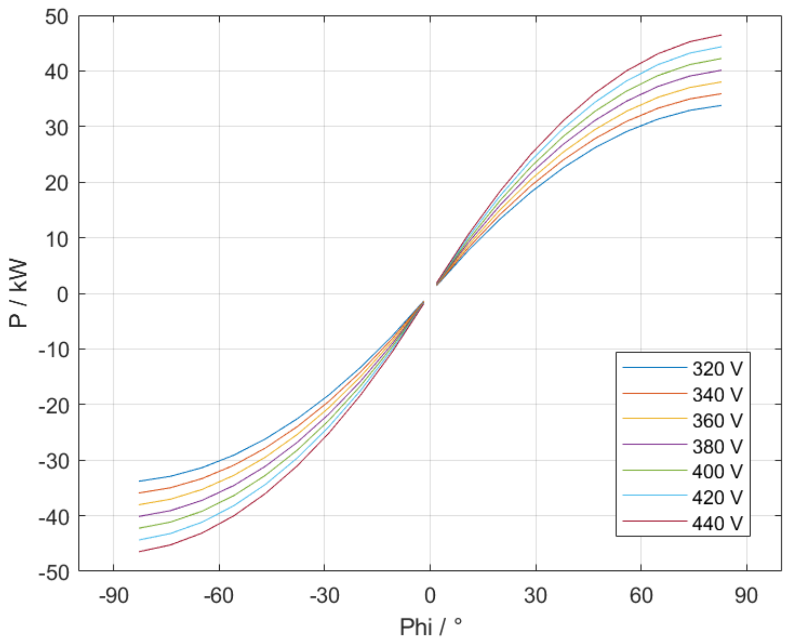

Figure 3: Power transfer curve for 1st design (Vin = 750 V, Vout = 320 V – 440 V, n = 0.6, Ls = 21 µH, fsw = 70 kHz).

With the value of the leakage inductance, the resulting current and voltage waveforms can be simulated for different operation points by using a simulation model of the DAB converter in PLECS. The simulation model can be observed in Figure 4.

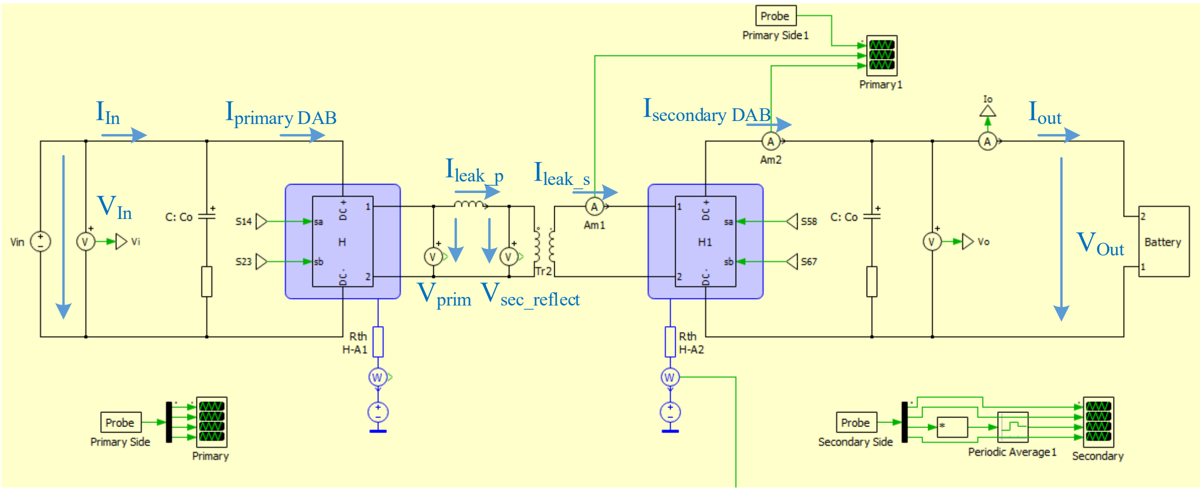

Figure 4: Simulation of the 22 kW Dual Active Bridge (DAB) converter. Ileak_p = leakage inductor current at the primary side; Ileak_s = leakage inductor current at the secondary; Iprimary_DAB = primary current DAB; Isecondary_DAB = secondary current DAB; Uprim = voltage full bridge primary; Usec_reflect = voltage full bridge secondary reflected to the primary; Uσ = Uprim-Usec = leakage inductor voltage; Iout = output current.

A thorough investigation has been done to obtain the maximum and minimum current and voltage values of the DAB. For the sake of simplicity, in this report only one operation condition will be presented. In Figure 5, the simulated waveforms of the DAB are presented for the following test conditions: V_{in} = 750 V, V_{Out} = 320 V, switching frequency = 70 kHz and power = 22 kW.

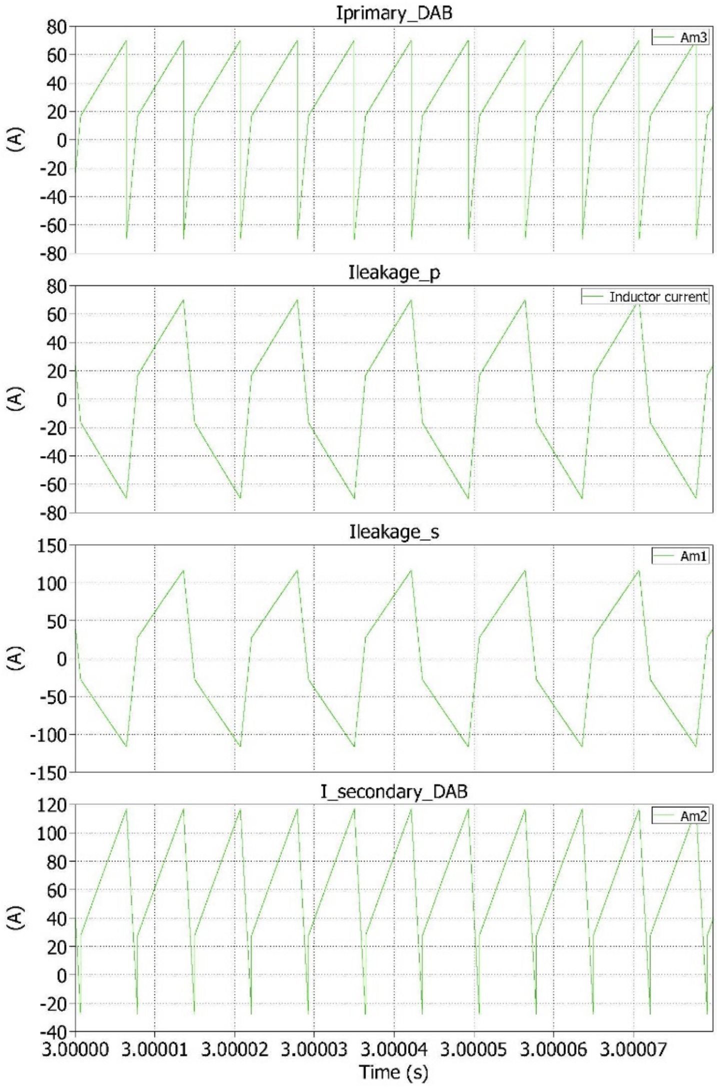

Figure 5: Simulated waveforms (II) of the Dual Active Bridge for the following testing conditions: Vin = 750 V; VOut = 320 V; fsw = 70 KHz; P = 22 kW.

The Dual Active Bridge simulation model was used to specify the components. For the semiconductors the following aspects are obtained:

- Maximum expected current through each semiconductor (MOSFET and diode)
- Maximum expected voltage of each semiconductor including over-voltages
- Maximum losses generated in each semiconductor

The simulation results can be observed in Figure 6 and Figure 7 for the primary-side and secondary-side semiconductors, respectively. The voltage and current waveforms of the MOSFET and diode have been simulated without including parasitic effects, and therefore, additional over voltages are expected in the real system. By comparing the currents of the primary and secondary H-bridges, it can be observed that the secondary H-bridge has higher current levels because of the lower voltage at the same power. This will have a direct implication on the power semiconductor lifetime, as it will be presented later.

In this project, power semiconductor modules have been preferred over discrete devices, since modules are used for the higher power range and are more affected by reliability issues (to be investigated in this project) than discrete devices. Therefore, the SiC MOSFET that has been selected for the DAB converter is a 1.2 kV/80 A SiC power MOSFET module in a half-bridge configuration, whose part number is BSM080D12P2C008. Figure 8 shows the open module that is used for the DAB converter, where three SiC MOSFET chips are placed in parallel. In total, four modules of this type are required for building the Dual Active Bridge converter.

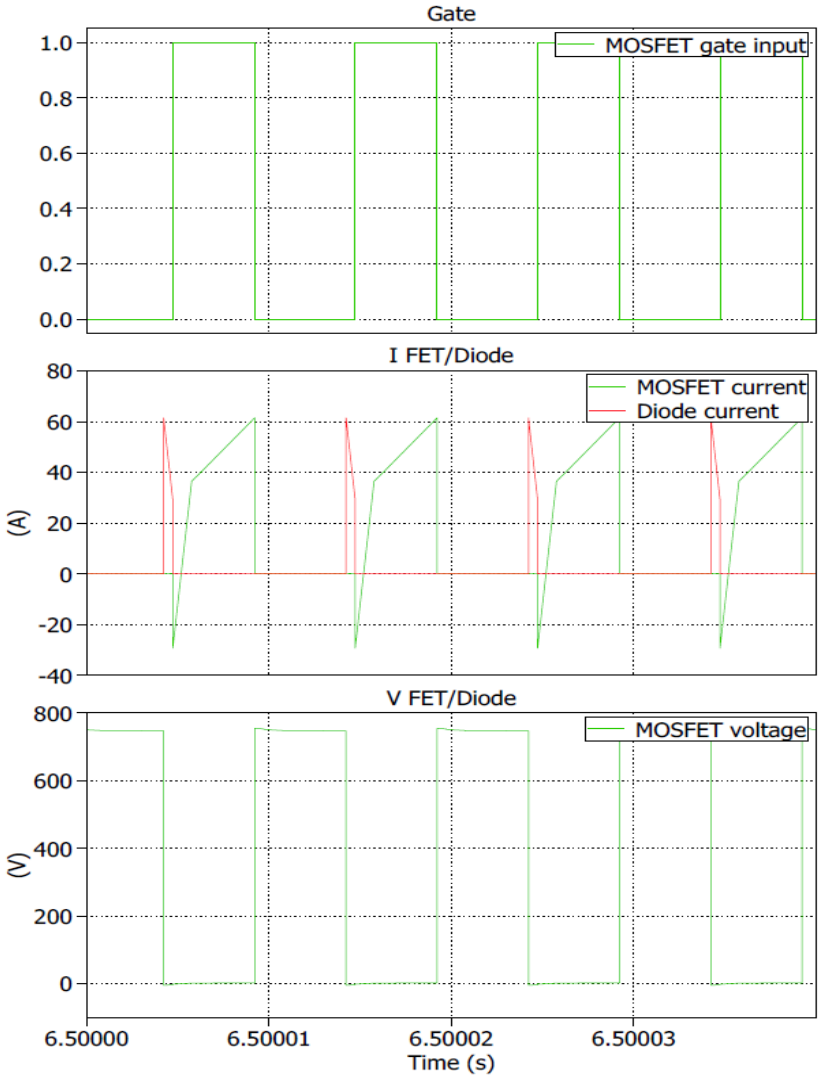

Figure 6: Voltages at and currents through the MOSFET and diode of primary side H-bridges at 22 kW and 25ºC.

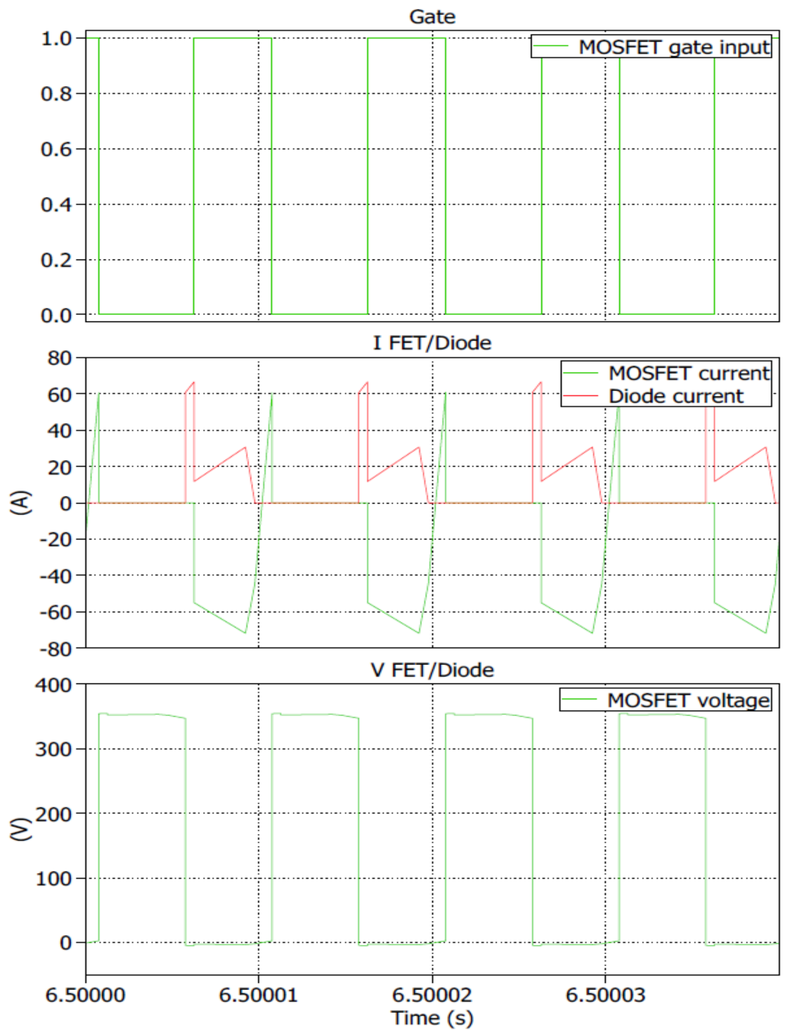

Figure 7: Voltages at and currents through MOSFET and diode of secondary side H-bridges 22 kW and 25ºC.

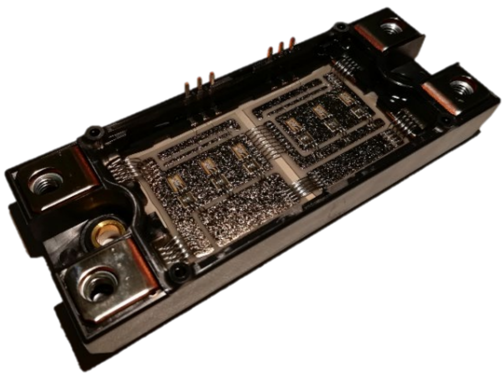

Figure 8: 1.2-kV/ 80-A SiC MOSFET power module in a half-bridge configuration (manufacturer: Rohm). The open module shows that three SiC MOSFET chips and three Schottky diodes are placed in parallel to achieve 80 A. In the DAB converter, such opened modules are used in order to monitor the junction temperatures during operation.

2.2 Selection of gate driver for the SiC power MOSFET module

The recommended gate driving voltages for silicon carbide power MOSFETs vary substantially among different manufacturers. In silicon-based power MOSFETs, the gate driving voltage is well established, where the typical values are V_{GS} = +15V/-10V. This is not the case for SiC power MOSFETs, since material defects that are only present in SiC material in combination with the thinner gate oxides have a negative impact on the gate oxide reliability. Therefore, the gate driving voltages must be adjusted for SiC power MOSFETs. For example, Rohm SiC MOSFETs are recommended to be operated at V_{GS} = +18V/0V - in contrast to CREE SiC MOSFETs that are recommended to be operated at V_{GS} = +20 V/-5V or even nowadays at VGS = +15V/-5V. Because of this reason, a customized two-channel gate driver has been developed at FHNW, where the gate voltage can be adjusted. The gate driver includes short circuit protection with soft-turn off function and adjustable turn-on/turn-off resistors. Active miller clamping is available for unipolar gate voltage use. shows the schematic of the two-channel isolated gate driver with highest flexibility for controlling SiC MOSFETs up to the 1200 V voltage class. Figure 10 shows a picture of the developed gate driver at the FHNW, whose specifications are:

- 1420 V isolation voltage
- V to 5.5 V input supply voltage
- Split outputs to provide 2.5-A peak source and 5-A peak sink current or with the external buffer circuit up to 15 A.
- Up to 2 W average power per semiconductor
- Adjustable gate voltage: e.g. +18V/0V or +15V/-5V
- Active miller clamp

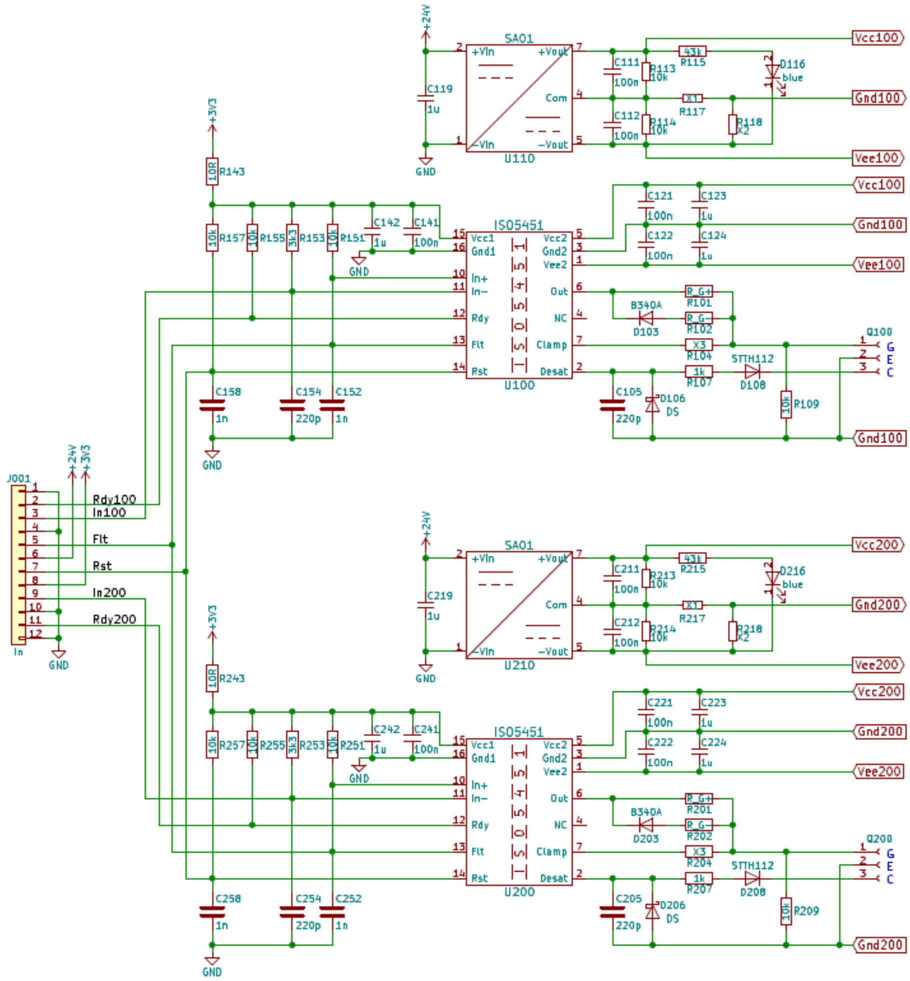

Figure 9: Schematic of the two-channel gate driver for 1.2-kV SiC MOSFETs.

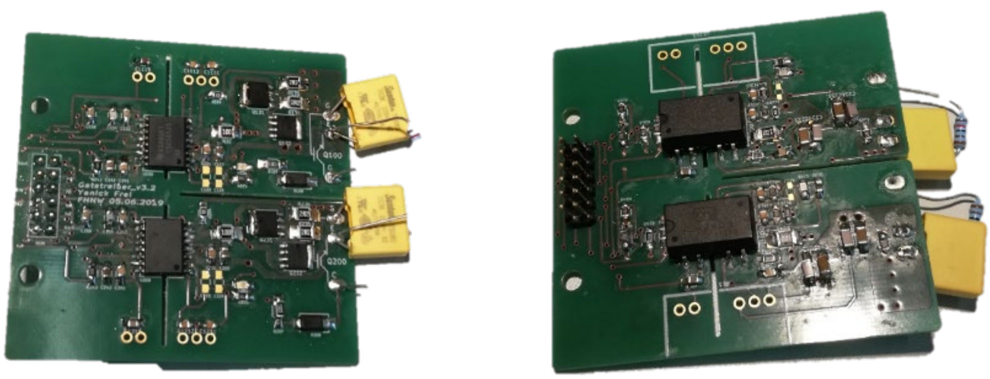

Figure 10: Photo of the FHNW gate driver board for 1.2-kV SiC power MOSFETs (top and bottom views).

3 Activities and results

3.1 Introduction

Operational tests have been carried out for the AC/DC and DAB DC/DC converter up to the nominal power of 22 kW. The efficiency has been investigated in detail for the DC/DC section, as shown in the following subchapters.

In addition, a reliability assessment of the semiconductors has been done. With the used model, the semiconductor lifetime in the DAB converter can be estimated. It has been refined by junction temperature measurements at different operation points. The model can be adapted to any other converter topology and it can be already used in a design phase for the optimization towards a more reliable converter.

During the commissioning, the progress of the project has been limited by following major factors:

Magnetic Components

Both of the two purchased series inductances failed during partial load tests. The self-developed gate unit detected the resulting overcurrent and safely turned off the semiconductors. The failed inductances were returned to the supplier; they are still under investigation at the manufacturer site. The manufacturer could not find a mistake in the design. Interestingly, the transformer lasted over all test campaigns up to nominal power. Therefore, the second (spare) transformer has never been used. Nominal converter power has been achieved, using a self-made toroidal air coil inductance that was built as a backup solution. It has been designed for functionality - i.e., to be able to fulfil the goals in this project and it was not optimized for efficiency. The converter efficiency drop using the self-made component is approximately 1 %, compared to early measurements operated at lower power with the purchased inductances. The maximum DAB efficiency therefore would rather amount to 96.58 % than 95.58 % with an optimized component.

Available Power Sources and Sinks

The maximum power to test the DAB converter is limited by the available voltage source to feed the DC link and by the power limitations of the voltage sink acting as a load. Both, an available DC supply and a sink are limited to 15 kW. Figure 1 further above shows that the DC link, which feeds the DAB converter, should be connected to the active rectifier developed by OST. During the first test campaign of the DAB converter, the active rectifier was under development and could not be used when the DAB converter was ready to be tested with higher power.

As soon as the AD/DC section including the mains filter was developed, tested and ready, the DC source and sink were connected in parallel to act as one sink that can sink the full power at the converter output. Hence, the pending tests could be finalized in a second test campaign.

Validation of the simulation model

As seen earlier (e.g. Figure 4), each operation point of the DAB converter can be simulated. Figure 11 shows good match between simulation and experimental results. The experimental results differ mainly because of high frequency noise on top of the fundamental waveforms due to parasitic effects.

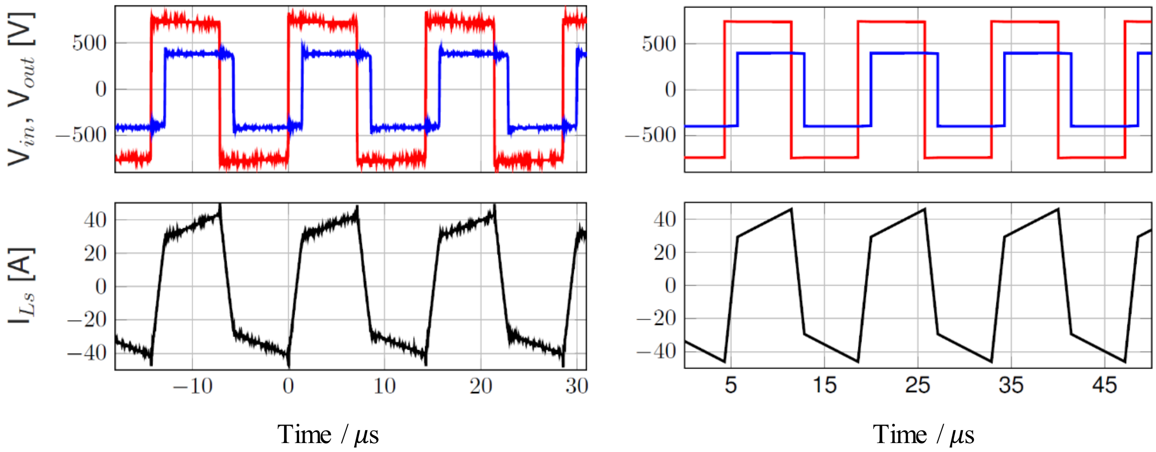

Figure 11: DAB converter waveforms: experiment (left); simulation (right). Operation point: Vin = 740V, Vout = 380V, Ls = 26 uF, Pin = 21 kW, Pout = 20.71 kW, fsw=70 kHz. Upper sub-figure: primary side full bridge voltage (red) and secondary side full bridge voltage (blue). Lower sub-figure: series inductance current.

With a good compliance, operation points can be pre-simulated in order to avoid dangerous operation points and damage of the hardware on one hand. On the other hand, other values of interest can be used out of the simulation any time without running a new measurement campaign in the laboratory. This is done for the reliability assessment of the semiconductors, as shown later in the report.

Efficiency measurement of the DAB converter

The efficiencies were measured using the measurement device DEWETRON 2600 available at OST. The powers were measured and calculated at the DC link input and the DC link output of the DAB converter. Because of this, no special sampling or bandwidth to measure fast fluctuating waveforms was required. For the total efficiency of the AC/DC and DC/DC stages, the input power has been measured at the three-phase input.

Accuracies:

For the current measurements, high precision current transducers Model LEM PM-MCTS 200 with shunt resistors of type PM-MCTS-BR5 with an amplitude accuracy of 0.05% were used. The shunt voltage was measured by a DEWETRON HIS-LV (Isolated low voltage module) with 200 mV input voltage range and an accuracy of ±0.02 % of the reading ±0.05 % of the range.

For the voltage measurements, DEWETRON HIS-HV (Isolated high voltage module) with 200 mV input voltage range and an accuracy of ±0.05 % of the reading ±0.05 % of the range was used.

Before each measurement campaign, all channels were calibrated. In Figure 12 and Table 2, the calculated efficiency is given for different operation points. The total measurement errors are calculated by means of error propagation of the individual measurement uncertainties. The corresponding error bars are given for each measurement point in the figure.

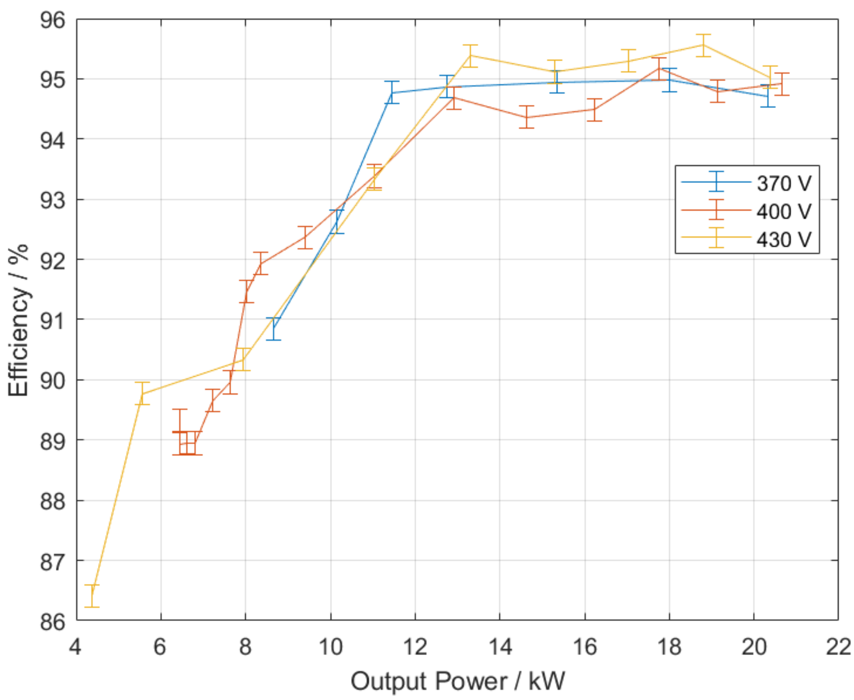

Figure 12: Total DAB converter efficiencies versus output power for different output voltages (EV battery state of charges) including absolute measurement errors.

For the depicted results, the DC link voltage at the input of the converter was supplied by the active rectifier and controlled to 720 V. The power was adjusted according to Figure 3, by the phase shift between the two full bridge voltages. This has been done for three different output voltages to emulate different SoCs of an EV’s traction battery. The maximum measured efficiency is 95.58%. Above one-third of the nominal power, the total converter efficiency is at 90% and higher. Figure 12 and Table 2 show the results.

Table 2: Operation Points and Efficiencies of the Dual Active Bridge Converter. The points of highest efficiency are marked red.

Vdc primary	Vdc secondary	Pin DAB / kW	Pout DAB / kW	Efficiency
720 V	370 V	9.52	8.65	90.86%
		10.97	10.16	92.62%
		12.07	11.44	94.78%
		13.44	12.75	94.87%
		16.17	15.35	94.93%
		18.95	18.00	94.99%
		21.45	20.32	94.73%
Vdc primary	Vdc secondary	Pin DAB / kW	Pout DAB / kW	Efficiency
720 V	400 V	7.25	6.45	88.97%
		7.22	6.45	89.34%
		7.45	6.63	88.99%
		7.66	6.82	89.03%
		8.05	7.22	89.69%
		8.48	7.63	89.98%
		8.78	8.03	91.46%
		9.10	8.37	91.98%
		10.19	9.41	92.35%
		11.81	11.03	93.40%
		13.63	12.91	94.72%
		15.51	14.63	94.33%
		17.17	16.22	94.47%
		18.65	17.75	95.17%
		20.20	19.14	94.75%
		21.77	20.66	94.90%
		22.99	21.43	93.21%
Vdc primary	Vdc secondary	Pin DAB / kW	Pout DAB / kW	Efficiency
720 V	430 V	5.05	4.36	86.34%
		6.21	5.57	89.69%
		8.79	7.94	90.33%
		11.82	11.03	93.32%
		13.95	13.31	95.41%
		16.07	15.29	95.15%
		17.87	17.02	95.24%
		19.68	18.81	95.58%
		21.44	20.37	95.01%
Vdc primary	Vdc secondary	Pin DAB / kW	Pout DAB / kW	Efficiency
750 V	400 V	21.16	19.98	94.42%
750 V	420 V	22.08	20.86	94.47%
700 V	400 V	19.51	18.46	94.62%

The measurement campaigns were not repeated several times in order to calculate statistical errors. However, one can clearly see that the data points of the efficiency measurements cannot be fitted to draw a smooth fitting curve that is inside the error bars. The reason for that is most likely oscillations on the DC link at the input as well as on the output of the DAB converter. Theoretically, these are DC values with additional ripples of the switching frequencies of the system. Because of parasitic components (inductances, capacitance) which cannot be avoided in a real converter, additional effects eventually appear. Common mode effects and system resonances cause unpredictable oscillations and noise that couple into measurements and converter parts besides "usual" EMC sources. The affected measurements can be those at the external ports of the converter, used to measure efficiency, as well as the measurements of the converter for its closed loop control. One example of a measurement with an oscilloscope with noise, ripples and resulting calculated efficiency is presented in the next figure for 750 V at the input, 420 V at the output and 20.86 kW output power.

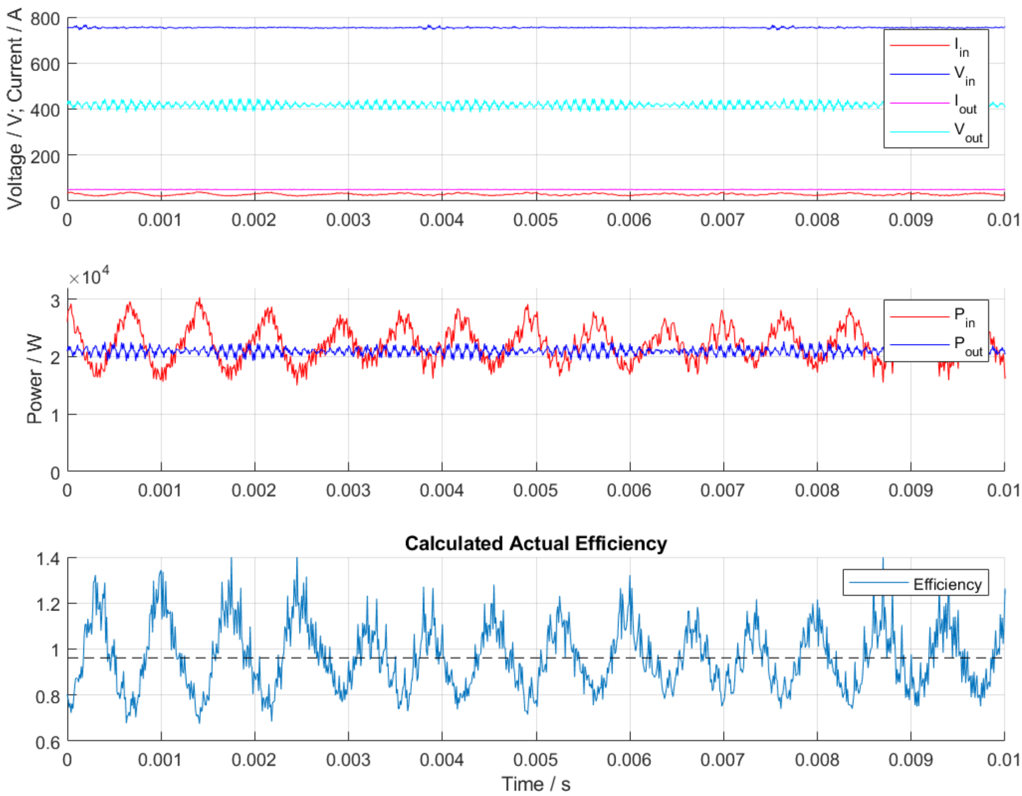

Figure 13: Measurement for DAB converter Input and output voltage and current in top graph. Calculated actual converter input and output power in the middle graph. Calculated actual converter efficiency and averaged efficiency (dotted line) in bottom graph.

The efficiency curves can be derived for each individual battery voltage from Figure 12. The additional estimated error is 0.35%. With this value, it would be possible to fit a smooth line. It is estimated out of the measurement points around V_{in} = 720 V, V_{Out} = 400 V, P_{out} = 6.45 kW, because more measurements were taken there.

3.4 Semiconductor losses versus DAB converter efficiency

The efficiency of the DAB is calculated according to equations below. The total converter losses $P_{loss,DAB,t}$ are calculated by adding the losses of the primary and secondary full bridges. $P_{sec,t}$ is the power on the secondary side of the converter during the corresponding time step. The losses of the magnetic components, DC link and other effects are not pre-calculated here.

$$\eta_t = \frac{P_{out,t}}{P_{in,t}} = \frac{P_{sec,t}}{P_{sec,t} - P_{loss,DAB,t}} \text{ for } P_{out,t} > 0 \text{ (charging battery)}$$

$$\eta_t = \frac{P_{out,t}}{P_{in,t}} = \frac{P_{sec,t} - P_{loss,DAB,t}}{P_{sec,t}} \text{ for } P_{out,t} < 0 \text{ (discharging battery)}$$

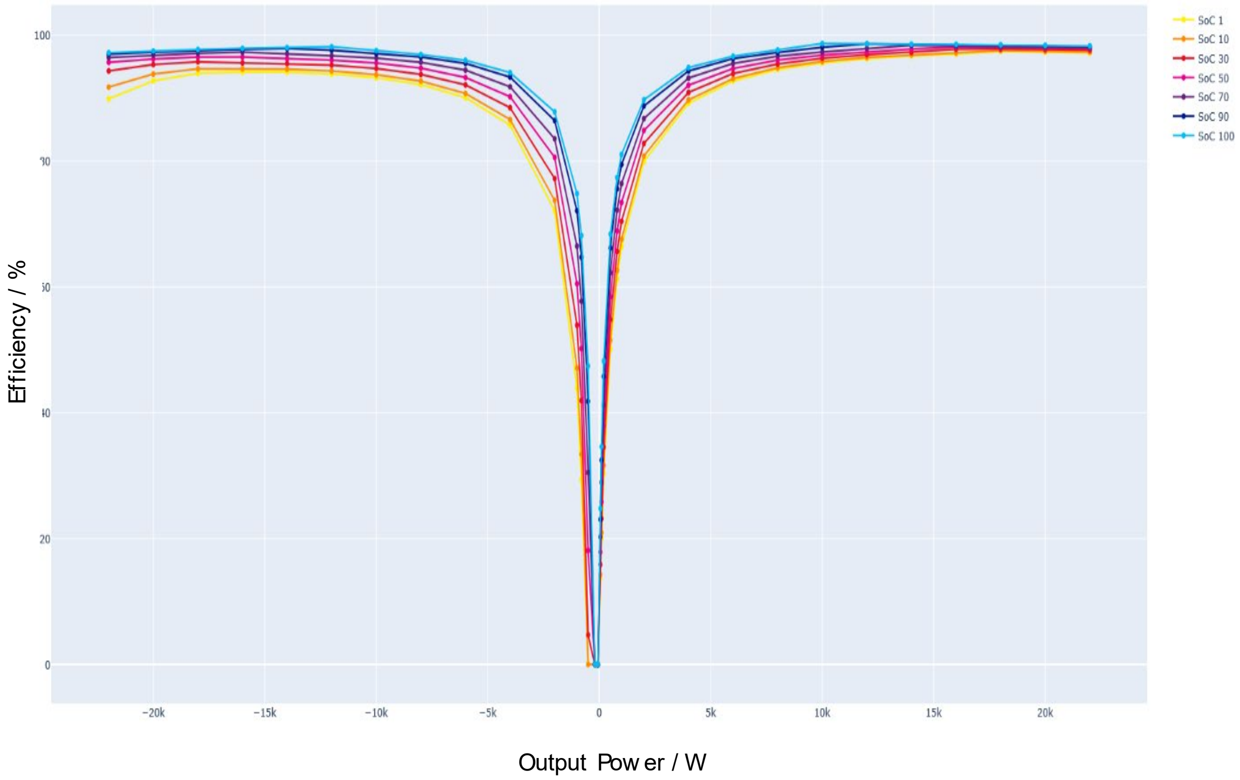

Figure 14: Efficiency calculation over the power range of the DAB converter (semiconductor losses only) for different battery SoCs.

In addition to the semiconductor losses, all other components add non-negligible losses as well. These are especially the magnetic components. Therefore, the efficiency measurements of the DAB converter show much lower efficiencies when compared to the calculated efficiencies of the semiconductors alone. The black curve in Figure 15 shows one efficiency curves considering semiconductor losses only.

In addition, the three measured efficiency curves for the entire DAB converter of Figure 12 are included. One can see that other components (e.g. the magnetic components) cause significantly more losses than the semiconductors and thus have a major impact on the total efficiency.

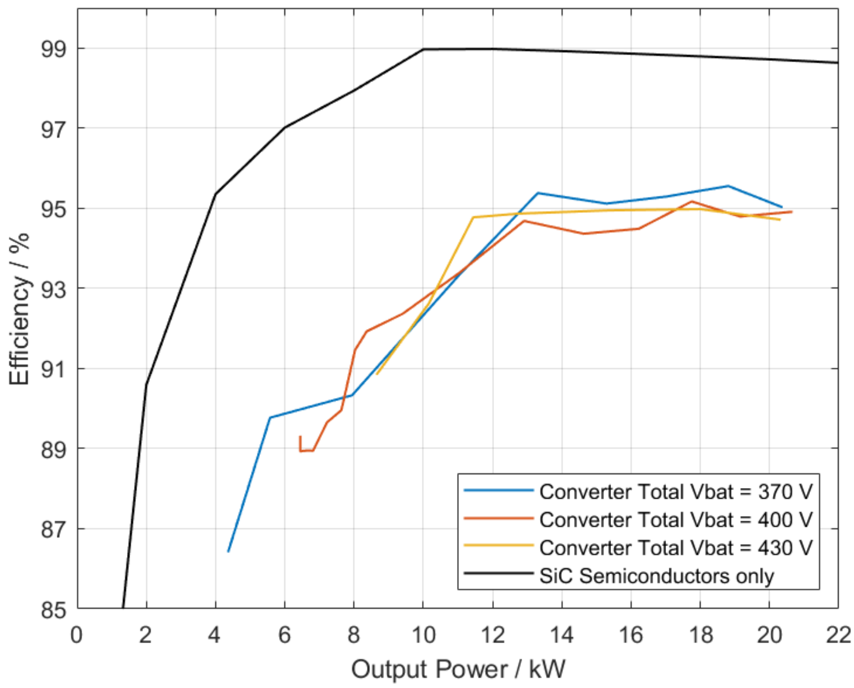

Figure 15: Calculated semiconductor efficiencies at different operation points versus measured total converter efficiency. It can be seen that in particular at higher power, the semiconductors only cause a minor part of the total losses.

This can also be noticed in the following infrared picture of the setup during the measurement, taken at 15 kW output power. The semiconductor temperatures are negligible considering the much higher temperatures of the magnetic components. The transformer shows the highest measured surface temperature of approximately 75°C, even 86°C at nominal power, whereas the semiconductors case temperatures are below 30 °C. The series inductance, which had failed during later tests, shows high temperature as well. However, the opening of the inductance is less visible on the infrared picture.

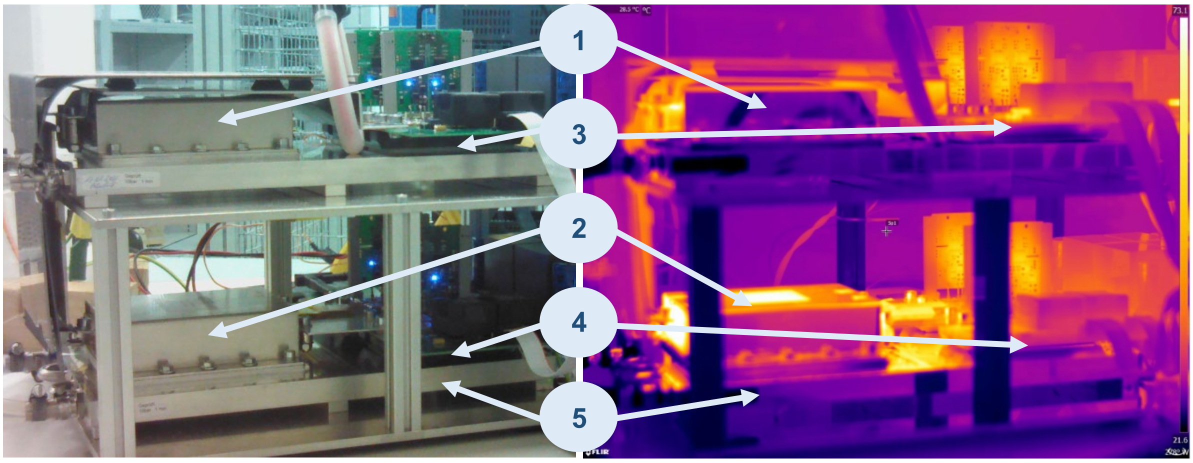

Figure 16: DAB converter during efficiency tests at OST (left); Infrared camera picture of the same view (right) at a power of 15 kW. (temperature colors reach from dark blue 21°C to white 75°C).

1. Series Inductance: purchased component (above); self-made component (below) with 40° maximum.
2. Transformer (shows the hottest temperature of the converter with 86°C)
3. SiC MOSFETs primary side (between PCB and heat sink)
4. SiC MOSFETs secondary side (between PCB and heat sink)
5. Heat sink

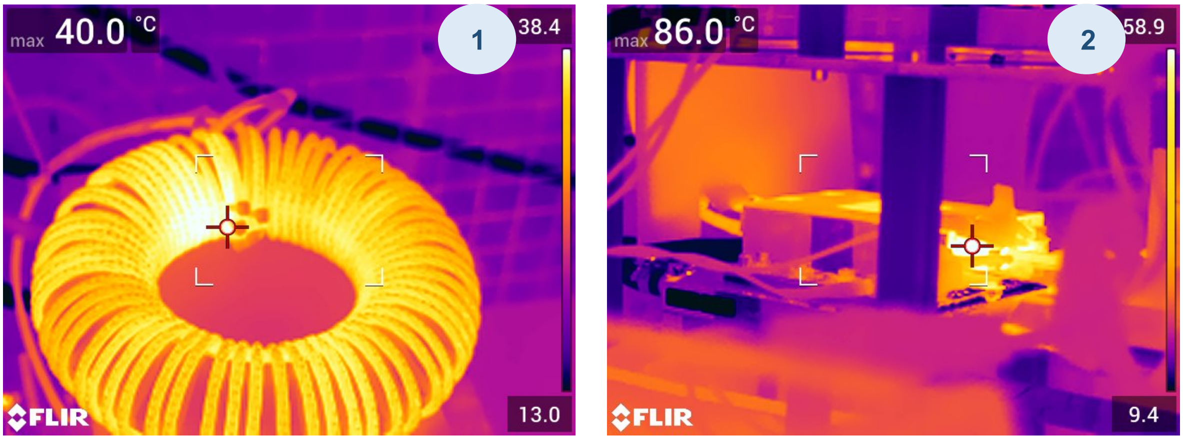

Figure 17: Infrared camera picture of the magnetic components during nominal power test (view from different angles). Self-made toroidal air coil under forced air cooling by a fan (left); transformer mounted on water cooler (right).

3.5 Calculated efficiency of SiC MOSFETs versus Si IGBTs

The efficiency and losses of the applied SiC MOSFETs operated in the DAB converter were calculated. The same can be done for other semiconductor types when the conduction and switching losses are known. With this procedure, the efficiency of SiC MOSFETs (Rohm BSM080D12P2C008; 1200 V / 80A) operated in the DAB converter is compared to the losses of silicon IGBTs (Infineon FS100R12W2T7; 1200 V / 100 A).

First calculations show that it would not be reasonable to simply replace the semiconductors and operate the converter at 70 kHz, since the IGBT switching losses would become unreasonably high (by more than a factor three). Therefore, the IGBT switching frequency is reduced to 10 kHz. To end up on the same power transfer curve as shown in Figure 3, the series inductance has to be increased proportionally. Figure 18 displays the adaptation and their consequences to make a fair and realistic comparison.

	Switching Frequency	
	10 kHz	**70 kHz**
SiC MOSFET (1200V 80A)	- Inductance increase proportionally - Size and losses of inductance and transformer increase Less semiconductor losses	**Actual Design** Prototype built and tested up to 22 kW
Si IGBT (1200V 100A)	Reasonable switching frequency Size and losses of inductance and transformer stay the same	Not reasonable

Figure 18: How to go from the actual converter design to a reasonable design using silicon IGBTs.

In Figure 19, the calculated converter efficiencies (considering semiconductor losses only) are depicted over the course of the converter output power. The black curve shows the efficiency with the calculated semiconductor losses of the actual design, presented already in Figure 15. With the increased inductance value and proportionally decreased switching frequency, the efficiencies are calculated for a converter using the SiC MOSFETs and the one using Si-IGBTs.

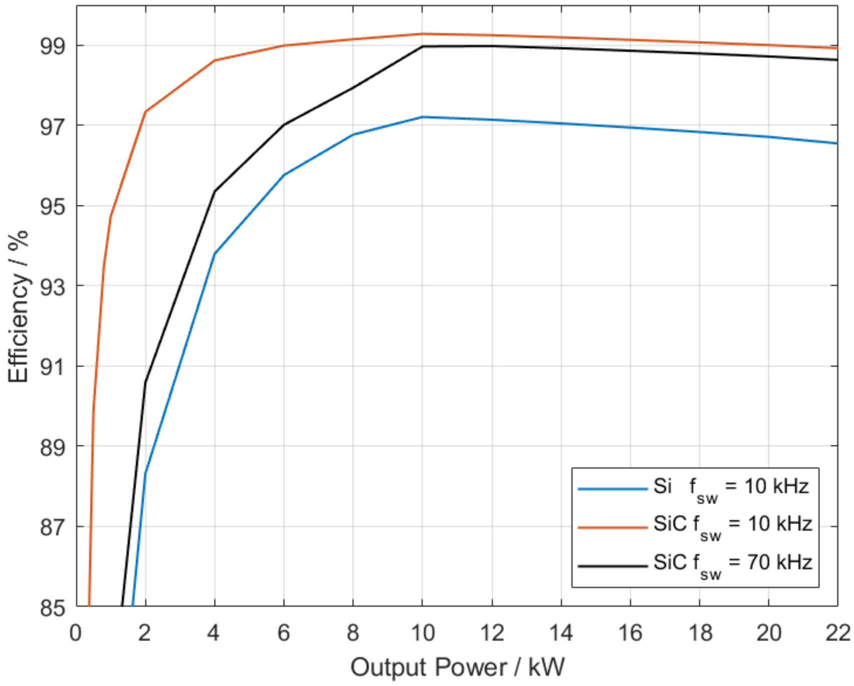

Figure 19: Calculated semiconductor efficiencies at different operation points. Comparison of efficiencies between Si-IGBTs and SiC MOSFET at 10 kHz and 70 kHz switching frequency.

3.6 Total AC/DC & DC/DC converter efficiency

The characterization of the DAB converter is shown and broadly discussed in the previous chapters. Finally, the total efficiency is summarized next by combining those measurements with the examined efficiencies of the input section from our partner OST, supplying the DAB input. The measurements of this AC/DC section and the data are discussed in detail in the report of the co-project SiCAa and are therefore not commented any further here.

Figure 20 shows the efficiency curve of the active rectifier, measured from the point of connection to the mains to the DC link that is charged up to a voltage of 750 V.

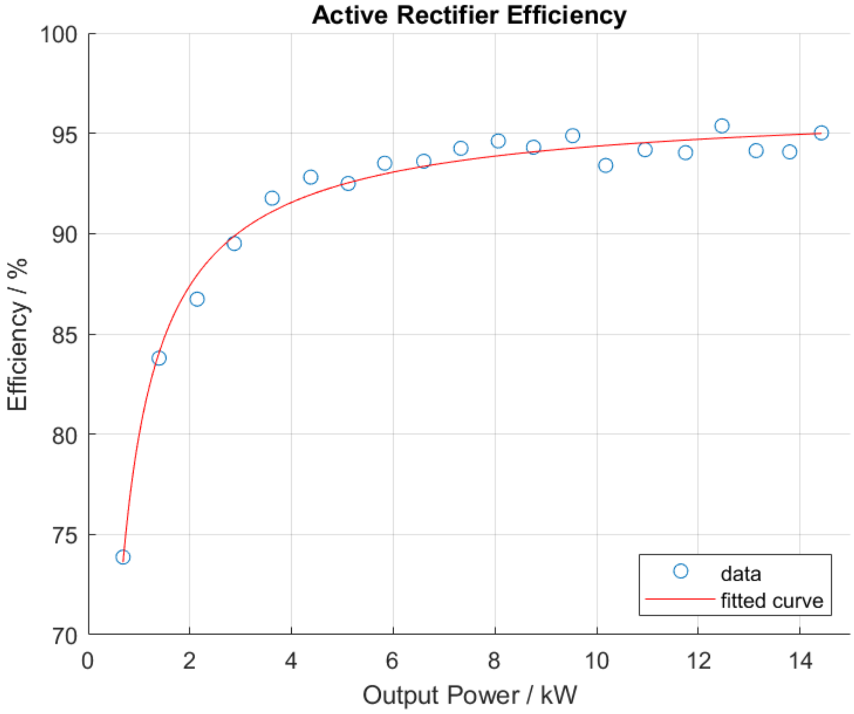

Figure 20: Efficiencies of active rectifier from mains connection point to DC link versus output power. Included are the data points and a fitting curve.

The data points are available up to an output power of 15 kW. The maximum efficiency is given at this power with 95 % with a rising tendency for higher output power. The co-project SiCAa is still ongoing and values can still change. For completeness, 95 % efficiency is used to calculate a total from the point of connection at the mains over the AC/DC and DC/DC section to the output where an EV battery could be connected.

Therefore, with 95 % efficiency from the input section and 95 % measured at the DAB, an overall efficiency of 90.25 % is achieved.

3.7 Discussion on efficiency

Silicon IGBTs do not reach as high switching frequencies compared to SiC MOSFETs, which makes a direct comparison between both semiconductor types difficult. In general, this is due to much lower switching losses and gate charge of SiC devices. From Figure 19, it can be seen that higher switching frequencies lead to lower efficiency in any of the semiconductor types due to the increased switching losses which are increased proportionally to the switching frequency. Therefore, two more curves have been added to the figure. If the converter is operated at a switching frequency of 10 kHz or lower, the DAB converter could be built using silicon IGBTs instead of SiC MOSFETs. The orange curve in Figure 19 shows the efficiency (semiconductor losses only) of a converter operated with SiC MOSFETs at 10 kHz switching frequency. The blue curve shows the efficiency (semiconductor losses only) of a converter that is operated with comparable Si IGBTs at 10 kHz switching frequency.

It is not reasonable to operate the built converter, with the magnetic components rated for 70 kHz, at 10 kHz for further comparison. The phase shift between the two H-bridge voltages then would become very small to transfer the power. Every two degrees of phase shift would already transfer 10 kW power. This can be seen in Figure 21 that shows the equivalent power transfer curves as shown in Figure 3, but with 10 kHz switching frequency and the series inductance of 25 µH up to 25 kW transferred power.

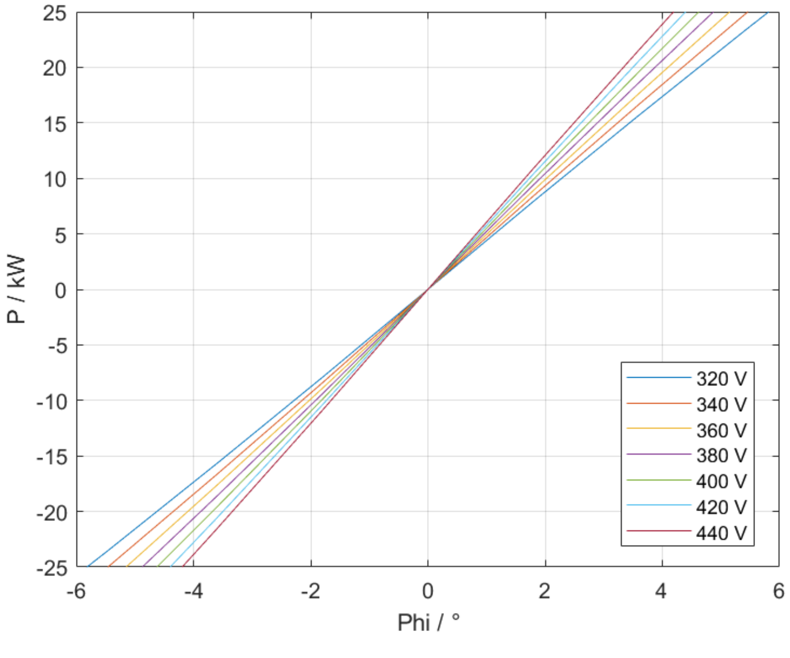

Figure 21: Power transfer curve for design (Vin = 750 V, Vout = 320 V – 440 V, n = 0.6, Ls = 25 µH, fsw = 10 kHz).

The voltage across the series inductance and the current waveforms would be different from the ones for 70 kHz. Since the operation point would be different, the losses in the components would not be comparable to 70 kHz switching frequency. Therefore, to end up on the same operation point and phase shift angle, the series inductor value must be increased by the same factor by which the frequency is reduced. Larger magnetic components cause higher losses since they are larger in size and weight.

Measurements that indicate the distribution of losses in each component were not carried out for several reasons, e.g. the availability of measurement and laboratory equipment and time. However, the actual losses distribution would be an interesting investigation. The component losses could be measured with an accurate measurement device to measure instantaneous input and output power electrically with a very high bandwidth for the 70 kHz signals. For water cooled components the losses could be also measured by calorimetric measures. Therefore, each component of interest should ideally be mounted on an individual heatsink.

Comparing the calculated losses of the semiconductors only, shows that SiC MOSFETs produce lower losses than IGBTs over the entire power range. This is also true for different switching frequencies of 10 kHz and 70 kHz. In partial load operation, SiC shows an even higher benefit when compared to full load.

Hence, when discussing efficiency of a converter or using SiC semiconductors to gain efficiency, **one has to keep in mind the other components and their effects to improve the overall converter efficiency**.

3.8 Control of the Dual Active Bridge

There are many control methods for such topology, one of the most common is the Phase Control Modulation (PCM). The DAB converter with PCM operates at a constant switching frequency where each switch is operated with 50% duty cycle to generate the square wave voltages on the primary and the secondary side bridges. The measured primary and secondary voltages of the DAB can be observed in Figure 22. By adjusting the phase-shift ratio between the rectangular voltage in the primary and in the secondary side bridges, the voltage across the series inductance will change. Thus, the power flow direction and magnitude can be controlled by controlling the phase shift. In Figure 22, the measured primary and secondary voltages as well as the resulting current across the leakage inductance is shown.

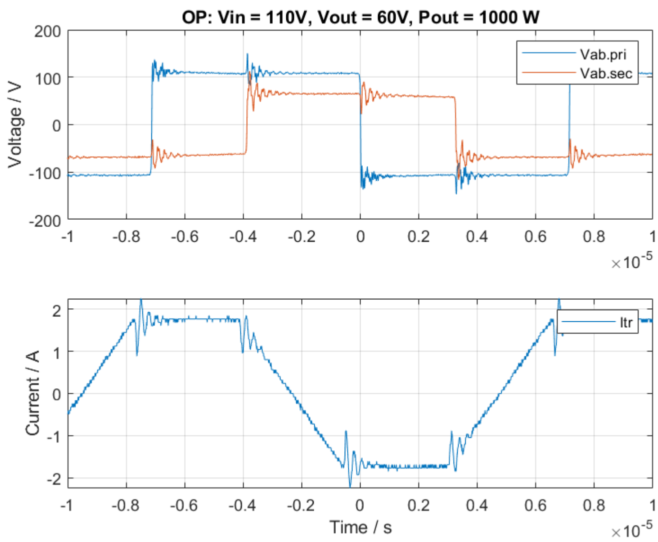

Figure 22: Measured primary and secondary voltages of the Dual Active Bridge converter (top) and current waveform across the leakage inductance (bottom).

Figure 23 shows the control block, where the power is measured and compared to a reference value. C1 and C2 are two feedback controllers designed for the outer (power control) loop and the inner (current control) loop respectively. The phase-shift ratio can be adjusted with a PI controller together with a feedforward algorithm. The feed forward block FF(P) provides a feed-forward phase shift φFF depending on the power setpoint. The feed forward algorithm contains the power transfer curves in a look-up table relating the power of the converter and the phase shift (refer to Figure 3).

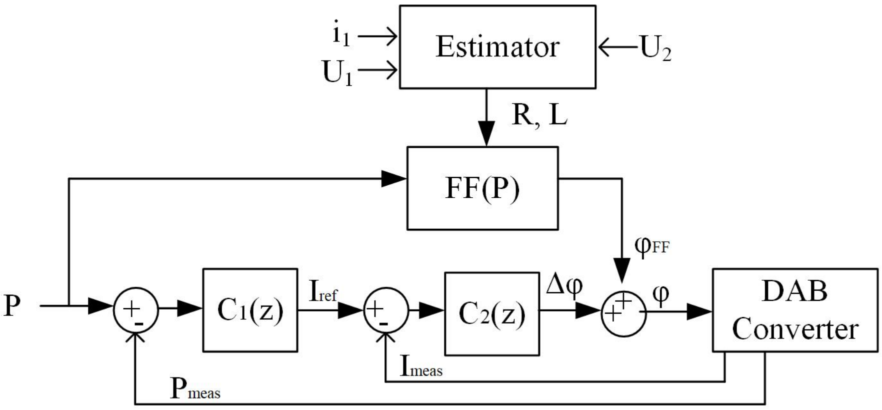

Figure 23: Control block diagram of the DAB converter [14].

The feed forward approach can facilitate the converter to generate fast response to reference steps comparing with a traditional PI control method.

Furthermore, in the frame of this project, an approximate analytical method to consider the effect the semiconductor's resistive losses, as well as the resistance of the transformer windings, for the phase control modulation of a Dual Active Bridge converter topology has been proposed. The new formula showing the relationship between the phase shift and the output power including the resistive losses is derived in [10].

One of the results of this work can be observed in Figure 24. Simulations have been done to compare the performance with and without loss compensation in the feedforward controller. It can be seen that the dynamic response with the loss-compensated feed forward is improved. This is because the phase angle computed with loss-compensation for a certain required output power already contains the estimated losses (resistive part in the output power formula). In case of feed forward based on lossless analysis, the feedback controller has to increase the computed phase angle to compensate the losses and other errors and therefore leads to a slower response. The feed forward scheme requires the parameters R and L, which can be estimated from measurements to improve the feed forward accuracy.

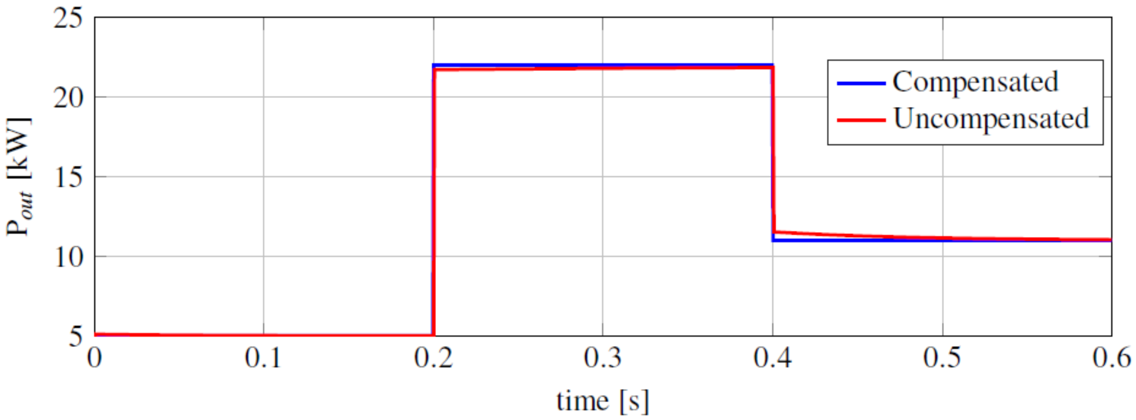

Figure 24: Simulated output power with uncompensated PCM controller and with compensated PCM controller [14].

3.9 Reliability assessment of the power semiconductors in the DAB

The goal of the design is achieving both high efficiency and high reliable operation. For the purpose of converter reliability estimation, a simulation model for a given mission profile (i.e., battery state of charge and converter power) is proposed to investigate the semiconductor thermal stresses that will determine the lifetime of the semiconductors.

Figure 25 shows the applied method to estimate the lifetime of the power semiconductor devices in our DAB converter [11, 12]. In a first step, an annual mission profile for the application of the converter in an EV with bidirectional functionality is generated (Figure 25, A). The mission profile contains the power output of the converter for every time step. It has a resolution (time step) of one minute. Information about the vehicle usage, the battery voltage etc. is required to generate the profile.

An electro-thermal model in PLECS has been used (Figure 25, B) to calculate the power losses of each device. The power loss look up table contains the power losses for every device (MOSFET, SBD for primary and secondary side) depending on the battery State of Charge (SOC) and the converter output power for given constraints, such as ambient temperatures [13].

By combining, the power losses look up table with the mission profile, the power losses for every time step are determined (Figure 25, D).

With the power losses and the thermal network (thermal impedances) of power modules and heat sink, the junction temperatures of the semiconductors are calculated (Figure 25, F).

The rainflow-counting algorithm is applied on the junction temperature profiles to determine the types of temperature cycles (degree of stress on a device) and the number of cycles for each type (Figure 25, G) [14].

A lifetime model that is well-known in the literature has been applied to estimate the number of cycles to failure. The lifetime of the whole converter equals to the shortest of the semiconductors' lifetimes (Figure 25, I).

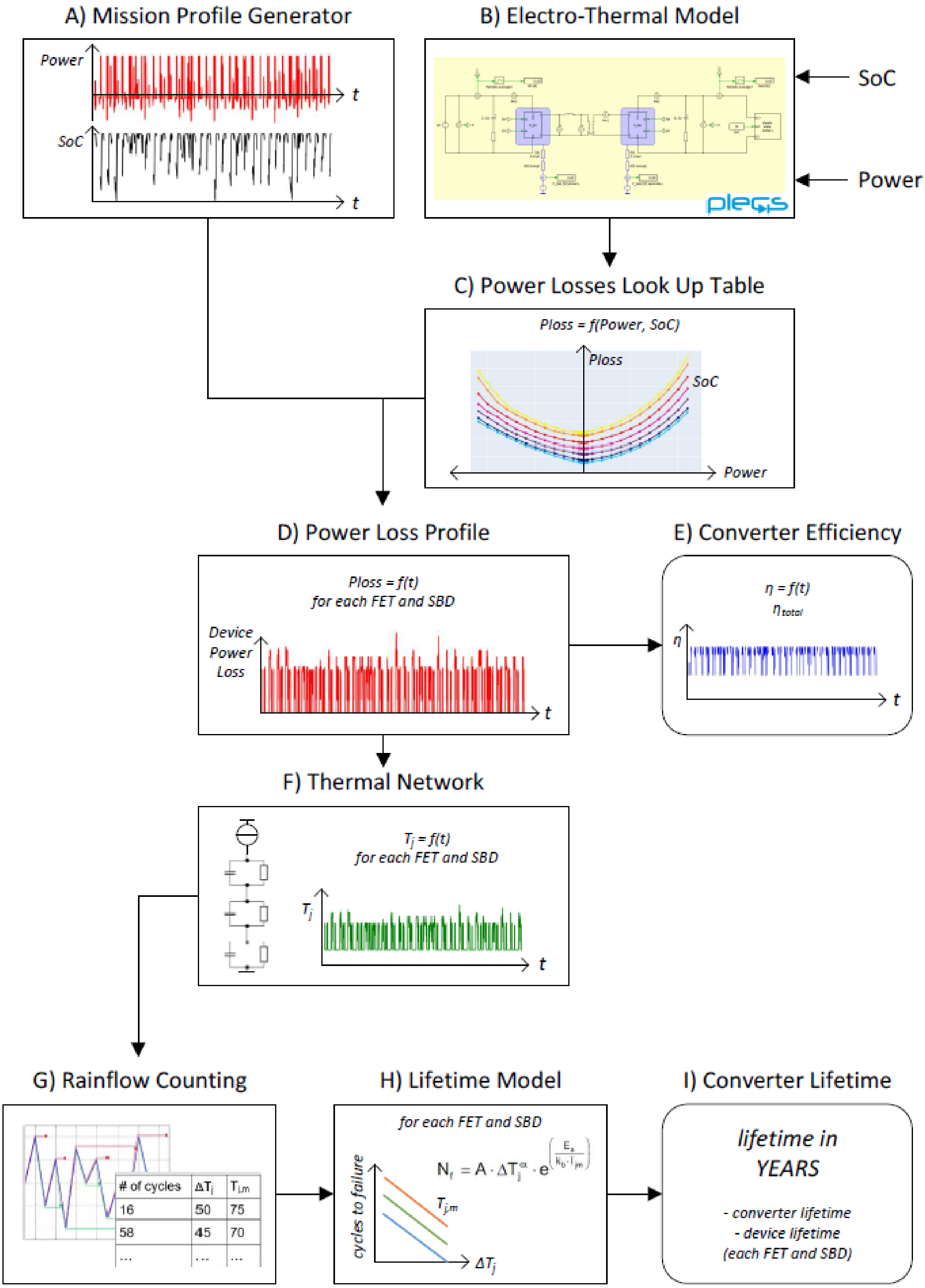

Figure 25: Applied mission-profile-based lifetime and efficiency estimation process.

3.9.1 Mission profile example

Figure 26 shows the generated one-year mission profile mentioned above (battery charger). The car is plugged out 35.5% of the time and plugged in 64.5 % of the time. When the car is plugged in, the battery is either being charged, discharged or available. Available means that the battery is fully charged and the house load is lower than the minimum load required to allow discharging.

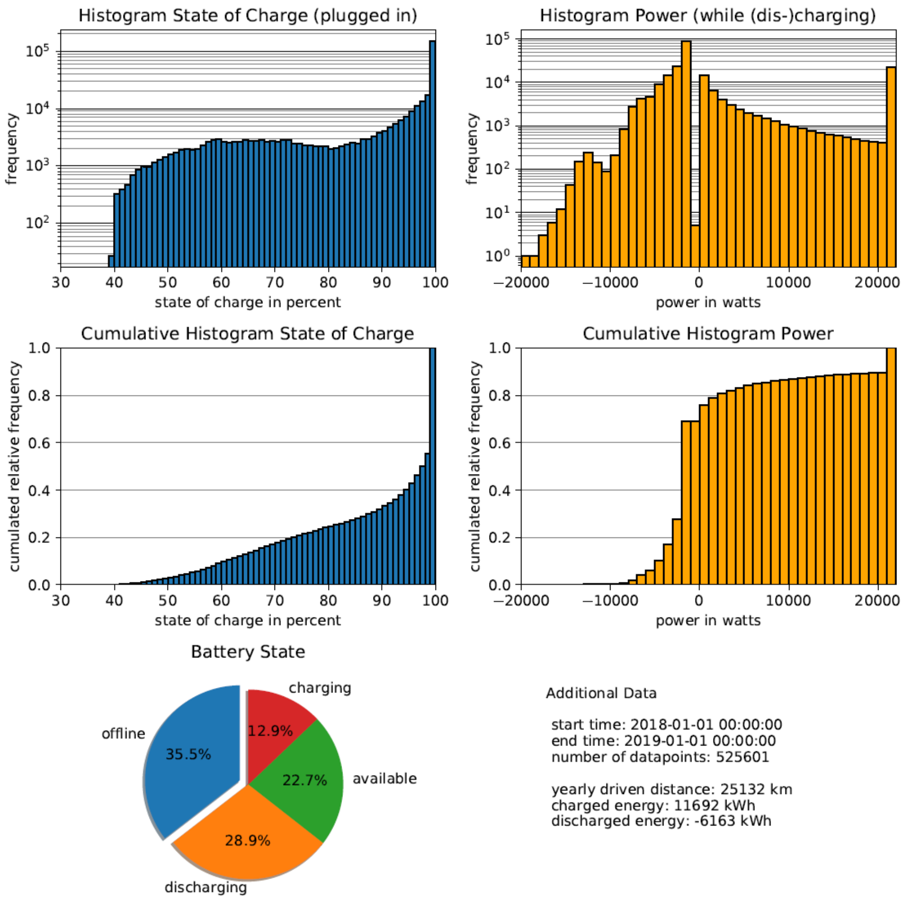

Figure 26: Summary of the generated mission profile. Top left: Histogram of the battery SoC. Center left: Cumulative histogram of the battery SoC. Bottom left: Pie chart indicating the battery state and whether the car is plugged in (charging, available, discharging) or not (offline). Top right: Histogram of converter power output (positive power = charging). Center right: Cumulative histogram of converter power output**. Bottom right: Additional data like driven distance and energy transfer.

3.9.2 Electro-thermal model results

The thermal model of the MOSFETs and diodes have been obtained from the manufacturer's datasheet. The PLECS simulation model has been modified to include the following data:

- Thermal impedance (Zth) containing thermal resistance (Rth) and thermal capacitance (Cth) from junction to case and from case to ambient.
- Conduction losses (for diode and MOSFET) depending on current and junction temperature
- Switching losses (for MOSFET only) depending on current, junction temperature and gate resistance

Figure 27 shows the power losses of the MOSFET and the diode for every combination of output power (positive means charging and negative means discharging) and battery SoC. The graph shows clearly that the primary and secondary devices are stressed to different degrees, which will lead to different temperatures. Devices with higher temperatures will be more likely to fail than the ones with lower temperatures and therefore have a shorter lifetime. One can see clearly that discharging the battery any further below a SoC of 30 % with full power will have an exponential increase in the junction temperatures of the secondary side MOSFETs and is not recommended at all. This is due to the low battery voltage and therefore higher currents. It would not be reasonable for the battery as well to further discharge it below a SoC of 20 % even with limited power to avoid deep discharge.

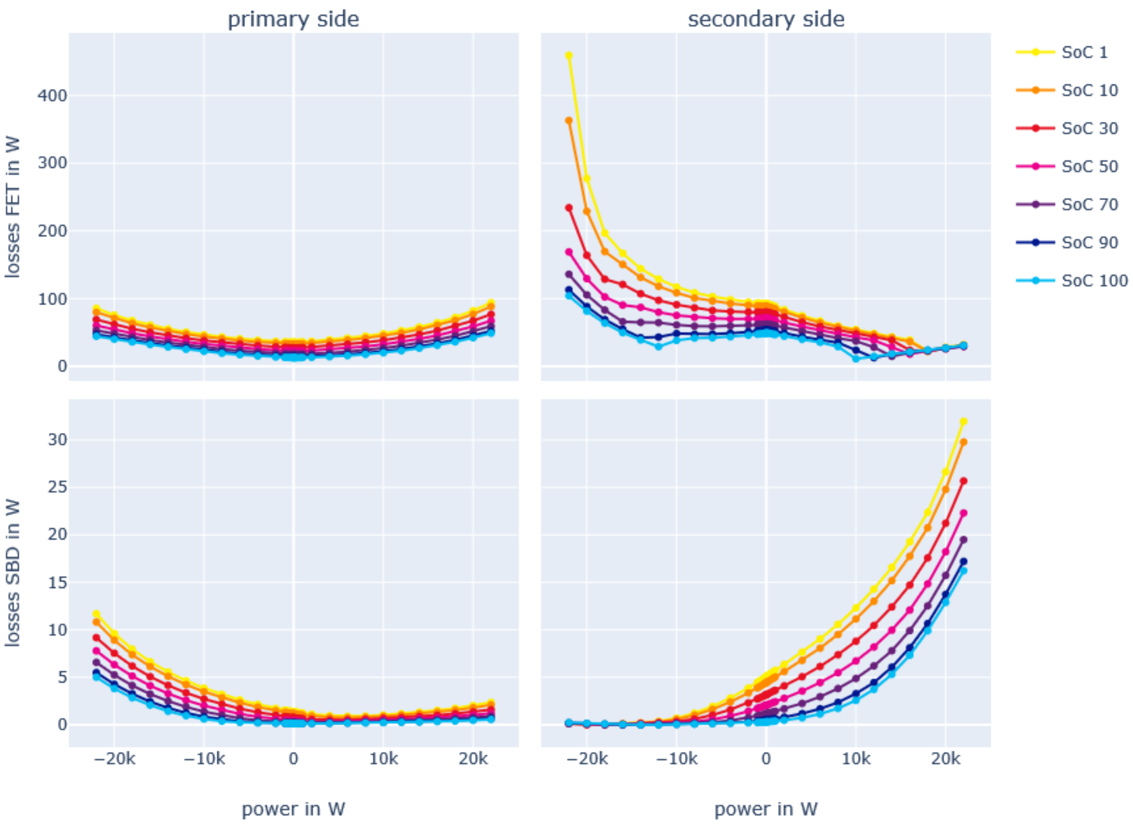

Figure 27: Power losses depending on output power and battery SoC. It is visible, that the devices on the primary side are stressed less than the ones on the secondary side.

Figure 28 shows the share of the total losses produced by each component type for a vehicle-to-grid (V2G) mission profile. The power MOSFETs on the H-bridge of the secondary side accounts for about 70% of the total losses.

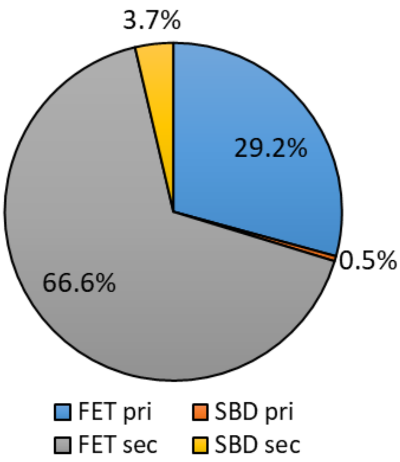

Figure 28: Share of the total converter losses produced by each component type in a V2G mission profile. "FET pri" stands for the four MOSFETs on the primary side of the DAB and "SBD pri" stands for the four Schottky Barrier Diodes on the primary side of the DAB.

3.9.3 Lifetime estimation

Recently, different lifetime models, which had originally been developed for Si semiconductors, have been tested for SiC [15]. The models (including the widely used LESIT model [16]) properly reflect power cycling test results for large junction temperature swings ΔTj, but they all underestimate the lifetime for values of ΔTj ≤ 60 K. This means that a lifetime model of SiC, which is validated for the entire ΔTj range, is not yet in place. A lower boundary for the lifetime of a SiC device can be given.

Despite of this, to obtain a *first rough estimation* for the SiC semiconductor lifetimes in the developed DAB converter, the LESIT model has been applied to estimate the number of cycles to failure Nf. It is an empirical model that does not distinguish between different failure mechanisms (bond-wire lift off or solder fatigue). The model was established by experimentally testing Si semiconductors under diverse operation conditions. The number of cycles to failure Nf (Equation 1) depend on the average junction temperature Tjm and the temperature difference ΔTj of the power semiconductor:

$$N_f = A * \Delta T_j^{\alpha} * e^{\left(\frac{E_a}{k_b * T_{jm}}\right)} \qquad (1)$$

Using the LESIT model, the lifetime of the SiC semiconductors in the DAB converter have been estimated for a mission profile with V2G functionality. The application of the DAB converter in an EV, even with V2G functionality, is not very stressful for the investigated power modules. When charging the battery, the power is usually constant for a long period (e.g. one hour) and slowly decreases towards the maximum SoC. This causes very few temperature cycles and therefore the power semiconductor devices. In stressful applications, the load profile changes in the range of milliseconds or seconds with high temperature swings. This could be the case in a photovoltaic inverter. When discharging the battery, the power has been assumed to deliver the power consumed by the house loads (up to 10 kW). This causes a few more thermal cycles, but still not enough to severely stress the power SiC MOSFET modules. The lifetime of the converter with the given mission profile has been estimated to be larger than 100 years, since the load changes a few times and very slowly, still resulting in a few temperature cycles and therefore in a large lifetime estimation.

3.10 Summary on the 22 kW bidirectional DC/DC SiC-based converter

3.10.1 Hardware and software design

A full-SiC 22-kW Dual Active Bridge (DAB) converter has been built with a DC input voltage of 750 V and a DC output voltage in the range of 320 V to 450 V. The Dual Active Bridge consists of two full bridges that are interconnected with a series inductance, and a medium frequency transformer.

As shown in Figure 29 below, the converter consists of the following main parts: four SiC MOSFET half-bridge power modules with voltage and current ratings of 1.2 kV and 80A; a planar series inductance of 21 µH; a planar transformer, whose transformers' turn ratio is 0.6; and two water cooled heatsinks for cooling the power modules and magnetics. A customized two-channel gate driver has been developed, including short circuit protection, soft turn-off function, and adjustable gate voltage. For the converter operation, the SiC MOSFETs have been operated with gate voltages of VGS = +18V/0V.

Two identical PCB boards have been developed: The first board includes the three-phase AC input, the connection to the AC/DC three-phase two-level SiC-based converter, the DC-link capacitors, the primary side H-bridge of the DAB converter and measurements needed for the control. The second board includes the secondary side of the Dual Active Bridge converter, the output capacitors, the DC output to the battery and the measurements needed for the control. The two PCB boards are identical to have a modular converter design, even if not all of the components have been mounted on the secondary board. This gives one more degree of freedom if further modifications are needed on the converter. An adaptation for futures 800 V EV traction battery voltage or an extension of the converter with an inverter to build a solid-state transformer is therefore possible.

As can be seen in Figure 29, the converter is connected to the real time controller RT BOX from Plexim through two interface boards (the analogue breakout board and the digital breakout board). The RT BOX is used for Rapid Control Prototyping (RCP) to provide the PWM control signals to the power semiconductor devices through the digital interface board. Via the analogue interface board, the voltage and current measurements are red. These measurements are needed for commissioning as well as to control of the DAB. Additionally, the silicon carbide power modules have been opened to allow the inspection of the junction temperature of the chip with the help of an optical fibre. This can be observed in Figure 30. The junction temperature was measured during the converter operation in order to validate the thermal simulation model in PLECS. With a precise simulation model, predictive maintenance and a more accurate reliability study of the DAB converter is possible.

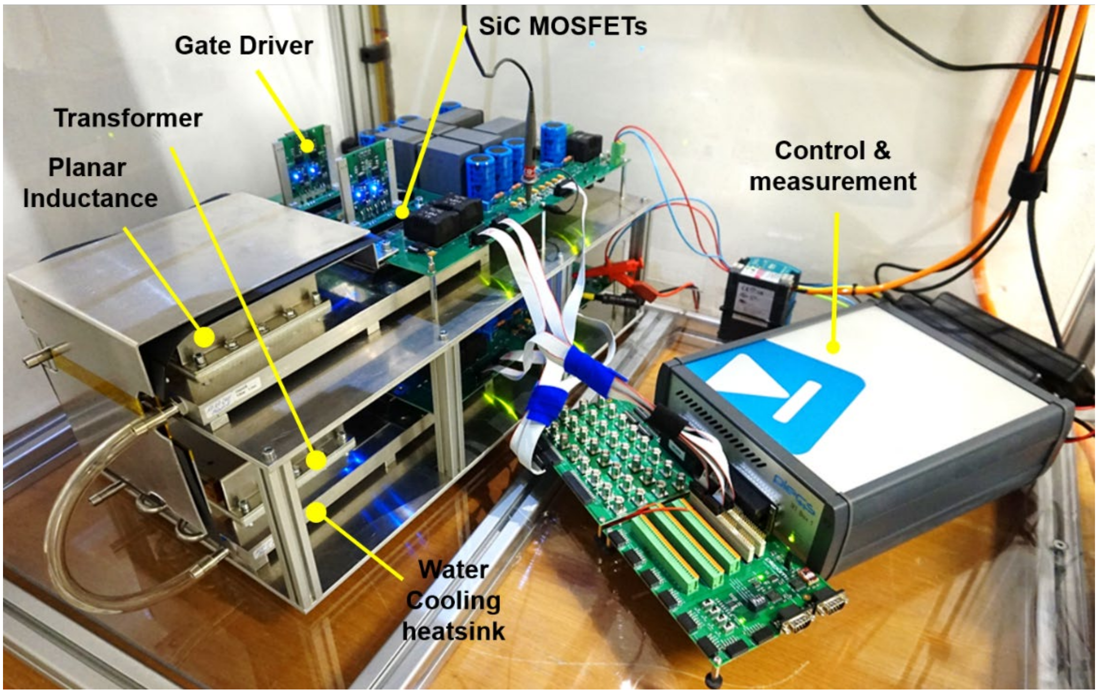

Figure 29: Picture of the 22 kW full-SiC Dual Active Bridge converter for an EV charger application.

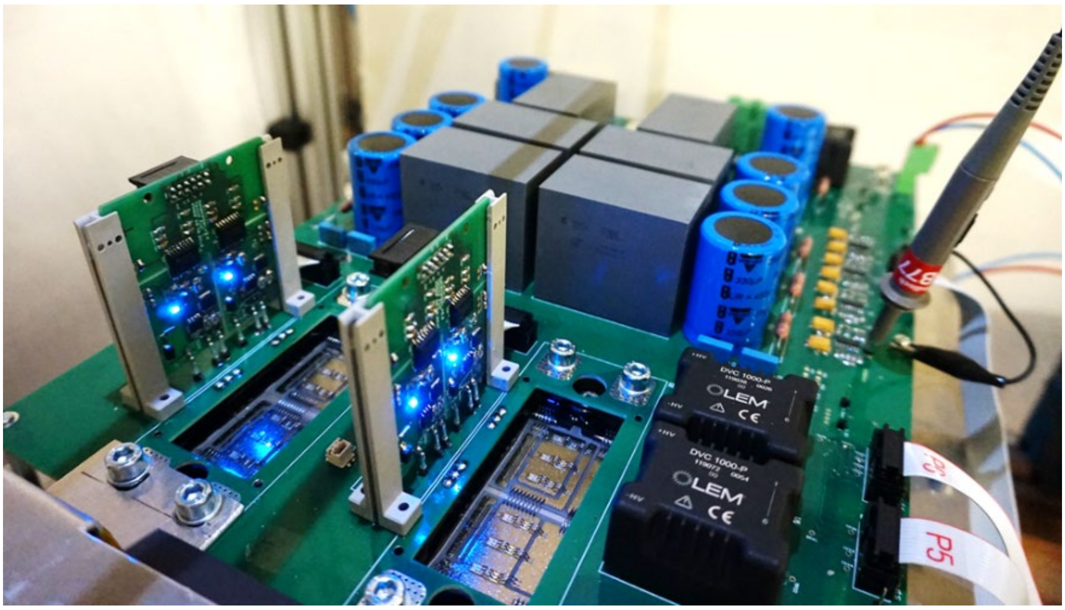

Figure 30: Zoom view of the primary board of the DAB. The inside of the SiC power modules can be seen through the opening in the green PCB.

The DC/DC Dual Active Bridge converter specifications can be observed in Table 1.

4 Evaluation of results

The conclusions are summarized in the following:

1. **Output power of the AC/DC & Dual Active Bridge Converter:** The converters have been successfully tested together up to the nominal power level of 22 kW.

2. **Efficiency measurement:** The efficiency of the DAB converter has been measured. **The highest measured total efficiency of the DAB is 95.58%.** When considering only the losses in the SiC MOSFETs, the efficiency can reach up to 99%. This means that the biggest fraction of the losses occurs in the passive components, in particular the magnetic components.

3. **Control improvements:** An approximate analytical method to consider the effect of the semiconductor's resistive losses, as well as the resistance of the transformer windings, for the phase control modulation of the Dual Active Bridge converter has been proposed. The proposed control scheme is planned to be implemented in the described 22 kW DAB converter.

4. **Reliability study:** A semiconductor lifetime simulation model of the DAB converter has been developed, to study the effect of the load profiles coming from a given mission profile. The presented case study is a lifetime estimation of a DAB converter for an onboard bidirectional battery charger for Electric Vehicles with vehicle-to-grid (V2G) functionality. The simulations show an uneven power loss distribution between the primary and secondary H-bridges of the DAB, with higher losses on the secondary side due to higher average current. This leads to a higher thermal stress of the secondary-side semiconductors, resulting in a shorter lifetime compared to the primary-side semiconductors. It has been also found that the V2G mission profile does not impose a high thermal stress on the semiconductors, which positively affects their lifetimes. The developed lifetime simulation model can be used to optimize the rating and cooling of the semiconductors for an optimal balance between cost and reliability before the hardware development process begins. However, for precise lifetime estimations, a validated lifetime model for SiC semiconductors needs to be established, which is currently under development in the SiC scientific community.

5. **Challenges with parasitic components:** The purchased magnetic components based on a planar technology have not resulted in a good solution. Both ordered inductances failed during the tests under partial load. The stray capacitances of the planar transformer cause strong capacitive coupling between primary and secondary side as well as to ground potential. The capacitance from primary to secondary side is 4.55 nF. This results in higher harmonics on either side as soon as there is a switching event on one of the H-bridges. Common mode currents appear because of the coupling to ground potential. In addition to that, the used semiconductor half bridge module package have a high internal parasitic inductance. Therefore, each switching event causes oscillations at the Drain-Source voltage and excites the passive network on the output of each H-bridge with all its parasitics and couplings. Snubber circuits at the semiconductors have been applied therefore. Nevertheless, snubber circuits as well as higher harmonic oscillations result in additional total losses in the system which are difficult to quantify. Hot spots inside the failed inductances, due to harmonics could be a possible reason for the malfunction. The part manufacturer did not comments on that.

6. **Efficiency and comparison of semiconductor types:** Silicon IGBTs do not reach as high switching frequencies compared to SiC MOSFETs and they do not necessarily need to. However, this makes a direct comparison on better efficiency between both semiconductor types difficult. A system or converter is designed and optimized to the needs of an application. Components are selected or even built accordingly. What can be said is that the magnetic components have a major impact on the total efficiency. In our case higher losses than the semiconductor losses. In most cases, if in an existing converter with silicon IGBTs, those are replaced with SiC MOSFETs, the energy efficiency of the converter will increase; especially in partial load operation. Converter efficiency optimization has to happen on converter level.

5 Next steps

The status and results are shown and discussed in this report. The project objectives have been achieved. The commissioning of the rectifier AC/DC converter to supply the DC/DC converter has been achieved, so that the DAB converter is supplied by the AC/DC converter for the operation at nominal power. The rectifier / inverter to feed motors is under promising commissioning, so that the round robin measurements can be carried out soon. That part is outside of the scope of this project, but part of the SiCAa co-project.

With the outcome of this project, further development and investigation of the DAB converter is of high interest to the FHNW Institute of Electric Power Systems. These are briefly discussed next.

5.1 Optimized magnetic components, suitable for fast switching slopes and low internal resonances

As in many converters, the magnetic components are always a critical part. Usually the higher the switching slopes (dV/dt) and / or frequency the more critical. As this report shows, the purchased inductances from a manufacturer have failed already at partial load, whereas the transformer performed well. Therefore, understanding magnetic components and the failure mechanisms as well as how to use that knowledge to build well-designed components for an application (energy, size, weight or cost efficient) is of high interest for all power electronics engineers.

5.2 Optimized control pattern for better efficiency and less harmonics

The standard phase shift control has its advantage in its simplicity. Nevertheless, this is not the most energy-efficient way to operate the converter. Disadvantages are that the soft switching region to turn on the semiconductors with low losses is limited and the turn-off happens at high currents, resulting in losses during switch off. In addition, the RMS currents, causing losses in all components, are depending on the phase shift in the standard control strategy. Several degrees of freedom (DC link voltage, output voltage, switching frequency, duty cycle of each full bridge converter etc.) can be adjusted for the optimization of the efficiency and waveforms shape in different operation points.

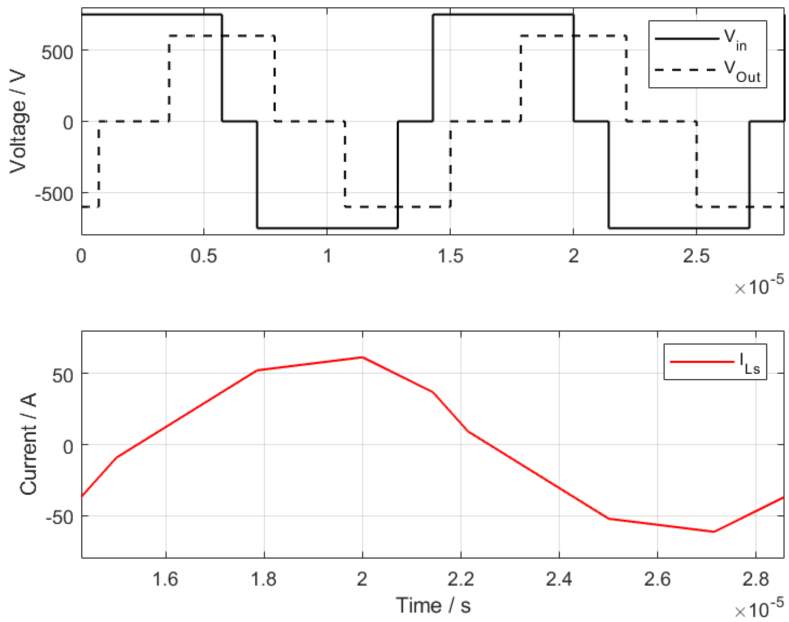

Figure 31: Example for the waveforms of another control strategy, where the duty cycle of each full bridge can be varied. Lower peak currents and different waveforms can be achieved.

5.3 Use the Hardware for higher frequency resonant converter topologies

With the hardware built in this project, especially the full bridge converter PCBs, other converter topologies can be derived. Resonant converters are highly interesting. They can have a very gain of the output voltage without using a transformer and in some applications, they can have less total converter losses than the DAB converter topology. Nevertheless, usually more complex control strategies are needed to operate such converters over a wider range of power.

6 National and international cooperation

During the development of the full SiC converter, several companies and partners have become aware of the outcome of this project work and show interest in collaboration with FHNW. Together with our other research areas in the field of silicon carbide converter design, its protection and control, we can offer and attract interesting and innovative research projects to partners in Switzerland and beyond.

Already acquired R&D projects in the field SiC; based on the experiences gained in the present project:

- Ampegon Power Electronics: Development project has started, funded by Innosuisse (Innovation Cheque) and Forschungsfonds Aargau.
- Reliability assessment of Si IGBTs and SiC MOSFETs in EV powertrains (funded by ECPE GmbH, Germany).

Furthermore, the collaboration between the FHNW and the OST has been strengthened. In addition to regular online meetings, usually every two weeks, the measurement campaigns were carried out together.

7 Publications

1. I. Pendharkar, T. Strittmatter, P. D. Reigosa and N. Schulz, "A Loss-Compensated Control Scheme for SiC-Based Dual Active Bridge Converter," 2020 22nd European Conference on Power Electronics and Applications (EPE'20 ECCE Europe), Lyon, France, 2020, pp. 1-8, doi: 10.23919/EPE20ECCEEurope43536.2020.9215762.

2. Abstract submitted and accepted for PCIM 2021; Title: “A Framework for Reliability Analysis of a SiC Converter for Automotive On-Board Charger Applications”.

8 References

[1] F. Krismer, Modeling and Optimization of Bidirectional Dual Active Bridge DC–DC Converter Topologies, PhD Dissertation, 2010.

[2] N. Soltau, H. A. B. Siddique and R. W. De Doncker, "Comprehensive modeling and control strategies for a three-phase dual-active bridge," 2012 International Conference on Renewable Energy Research and Applications (ICRERA), Nagasaki, 2012, pp. 1-6.

[3] Long term growth of the power electronics market is driving 300mm wafer-based production, Yole Development, 2019.

[4] M. Yilmaz and P. T. Krein, "Review of charging power levels and infrastructure for plug-in electric and hybrid vehicles," 2012 IEEE International Electric Vehicle Conference, Greenville, SC, 2012, pp. 1-8.

[5] L. Xue, Z. Shen, D. Boroyevich, P. Mattavelli and D. Diaz, "Dual Active Bridge-Based Battery Charger for Plug-in Hybrid Electric Vehicle With Charging Current Containing Low Frequency Ripple," in IEEE Transactions on Power Electronics, vol. 30, no. 12, pp. 7299-7307, Dec. 2015.

[6] D. Aggeler et al., "Bi-Directional Isolated DC-DC Converter for Next-Generation Power Distribution - Comparison of Converters using Si and SiC Devices," *2007 Power Conversion Conference - Nagoya*, Nagoya, 2007, pp. 510-517.

[7] Wolfspeed, https://www.youtube.com/watch?v=iwsgQnitiis

[8] Wolfspeed, https://www.youtube.com/watch?v=VWg2glkMIXo

[9] Xun Gong and Jayanth Rangaraju. "Taking charge of electric vehicles – both in the vehicle and on the grid", Texas Instruments application note.

[10] I. Pendharkar, T. Strittmatter, P. D. Reigosa and N. Schulz, "A Loss-Compensated Control Scheme for SiC-Based Dual Active Bridge Converter," 2020 22nd European Conference on Power Electronics and Applications (EPE'20 ECCE Europe), Lyon, France, 2020, pp. 1-8.

[11] P. D. Reigosa, H. Wang, Y. Yang and F. Blaabjerg, "Prediction of Bond Wire Fatigue of IGBTs in a PV Inverter Under a Long-Term Operation," in IEEE Transactions on Power Electronics, vol. 31, no. 10, pp. 7171-7182, Oct. 2016.

[12] D. Hirschmann, D. Tissen, S. Schroder, and R. De Doncker, "Reliability prediction for inverters in hybrid electrical vehicles," IEEE Trans. Power Electron., vol. 22, no. 6, pp. 2511–2517, Nov. 2007.

[13] J. McPherson, Reliability Physics and Engineering, 2nd ed. Switzerland: Springer Int., 2013.

[14] M. Miner, "Cumulative damage in fatigue," J. Appl. Mech., vol. 12, pp. 159–164, 1945.

[15] F. Hoffmann, N. Kaminski, "Power Cycling Capability and Lifetime Estimation of Discrete Silicon Carbide Power Devices," Materials Science Forum, vol. 1004, pp. 977-984, 2020.

[16] M. Held, P. Jacob, G. Nicoletti, P. Scacco, and M. Poech, "Fast power cycling test of IGBT modules in traction application," Proc. of the 2nd Int. Conference on Power Electronics and Drive Systems, Vol. 1, pp. 425-430, 1997.